ELSEVIER

Nuclear Physics B 460 (1996) 3-36

NUCLEAR PHYSICS B

Production of neutral pseudo-Goldstone bosons at LEP II and NLC in multiscale walking technicolor models

Vittorio Lubicz [a], Pietro Santorelli [b]

[a] *Department of Physics, Boston University, 590 Commonwealth Avenue, Boston, MA 02215, USA*

[b] *Dipartimento di Fisica, Università di Napoli "Federico II" and INFN, Sezione di Napoli, Mostra d'Oltremare, pad 19-20, I-80125 Naples, Italy*

Received 19 May 1995; revised 31 July 1995; accepted 6 December 1995

Abstract

Walking technicolor (WTC) models predict the existence of heavy neutral pseudo-Goldstone bosons (PGBs), whose masses are typically expected to be larger than 100 GeV. In this paper, we investigate the production and decay of these particles at the high energy e^+e^- experiments, LEP II and NLC.

We find that, in WTC models, the production of neutral PGBs can be significantly enhanced, by one or two orders of magnitude, with respect to the predictions of traditional (QCD-like) TC models. The origin of such an enhancement is the existence of several low energy TC scales, that are likely to appear in WTC theories. This could allow the PGBs to be observed even at the energy and luminosity of the LEP II experiment. At LEP II, the PGBs are expected to be produced in the $e^+e^- \to P\gamma$ channel, and, possibly, in the $e^+e^- \to Pe^+e^-$ channel, with a total rate that can be of the order of several tenths per year. Due to the typical large values of PGB masses, the relative branching ratios of PGB decays, in WTC theories, are different from those predicted in traditional TC models. In particular, a large fraction of these decays can occur in the $P \to \gamma\gamma$ channel. In considering the PGB production, at LEP II, we find that, in most of the final states, the distinctive signatures of WTC events should allow the Standard Model background to be reduced to a negligible level. We also find that, at a 500 GeV NLC experiment, the production of neutral PGBs can occur in several channels, and can be of the order of 10^3 events per year. Instead, when we consider traditional TC models, we find that no PGB are typically predicted to be observed, both at LEP II and the NLC experiment.

SSDI 0550-3213(95)00644-3

1. Introduction

One of the most general predictions of any theory of dynamical electroweak symmetry breaking and, in particular, of its most popular realizations, technicolor (TC) [1]-[3] and extended technicolor (ETC) [4,5] theories, is the existence of a large number of pseudo-Goldstone bosons (PGBs). In all non-minimal TC models, for example, several tenths or even hundreds of these particles are expected to exist, and the lightest of these states should probably have sufficiently small masses to be produced in current or presently planned experiments. Therefore, the experimental searching of PGBs is a powerful tool in order to investigate the nature of the electroweak symmetry breaking.

Over the last years, within the framework of traditional TC models, the production of PGBs has been considered in a series of papers [6]-[9], both at hadron and lepton colliders. It is known, however, that, in the attempt to correctly describe the ordinary fermion mass spectrum, traditional TC models typically lead to large flavour changing neutral currents (FCNC) [5,10], which are not suppressed to a phenomenologically acceptable level. For this reason, most of these models are actually ruled out by the experimental data.

In addition, traditional (QCD-like) TC models present problems with precision electroweak tests. The electroweak radiative correction parameter S, for example, typically receives positive contributions in these theories, and these contributions grow with the number of technifermion doublets [11]. Experiments, however, seem to find S to be very small or even negative [12].

Several years ago, walking technicolor (WTC) theories [13] have been proposed as a natural solution to the FCNC problem of TC. The WTC idea is simple. In WTC theories, the running of the TC coupling constant, α_{TC}, between the TC scale Λ_{TC} and, approximately, the ETC scale Λ_{ETC}, is very slow. Consequently, the TC interactions remain strong enough over a large range of momenta, and the values of the technifermion condensates, renormalized at the scale Λ_{ETC}, are significantly enhanced. This enhancement also increases the values of the ordinary fermion and technifermion masses, generated at the scale Λ_{ETC}. Thus, in WTC theories, Λ_{ETC} can be raised to several hundred TeV, and the ETC-generated FCNC are properly suppressed.

In addition, WTC theories are not necessarily invalidated by precision electroweak tests [14]. In these theories, radiative corrections to the Standard Model parameters are difficult to be reliably estimated [15], mainly because the mass spectrum of WTC cannot be simply obtained by scaling QCD data at higher energies. It has been argued, however, that in WTC the value of the electroweak parameter S could be smaller than the value estimated in traditional TC models, and deviations from the Standard Model may fall within current experimental bounds [16].

In this context, it is important to investigate whether signatures of WTC theories might be detected in current or presently planned experiments. In this paper, we have considered the production and decay of PGBs, in WTC theories, at the high energy e^+e^- colliders, LEP II and NLC. The phenomenological analysis performed in this paper has been partially inspired by the work of Ref. [17], in which WTC signatures, at hadron

colliders experiments, have been extensively studied. The relevant result of Ref. [17] is that, although most of the experimental signatures for TC at hadron colliders have long been regarded as very difficult to detect [6], however, the same consideration does not apply to models of WTC. In this paper, we reach a similar conclusion: in WTC models, the PGBs production at high energy lepton colliders can be significantly enhanced, by one or two orders of magnitude, with respect to the predictions of traditional, QCD-like, TC models. In particular, this enhancement could allow the PGBs to be observed even at the energy and luminosity of the LEP II experiment.

In order to qualitatively understand this enhancement, we observe that two features of WTC dynamics play, in this respect, a significant role. On one hand, the enhancement of technifermion condensates, characteristic of WTC, also raises the PGB masses, relative to their typical values in QCD-like TC theories. Thus, one finds that, in WTC theories, the masses of the lightest PGBs are expected to be larger than approximately 100 GeV, whereas typical masses of the order of 40 GeV are predicted to be found in traditional TC models [5]. Incidentally, this also means that, if TC is walking, the PGBs are likely to be too heavy to be produced at the LEP I or SLC experiments.

On the other hand, several low energy TC scales are expected to exist in WTC models. Multiscale TC models have been proposed in fact as a natural way to implement a walking coupling [19]. In multiscale TC models, the slow running of α_{TC} is due to the existence of a large number of technifermions. Typically, many technifermions belong to the fundamental representation of the TC gauge group, while few technifermions may enter in higher-dimensional representations. If this is the case, different values of the technipion decay constants, F_i, are also expected to exist, depending on the representations to which the corresponding technifermions T_i belong [20]. Since the largest TC scale is bounded above by the characteristic scale of electroweak symmetry breaking, $F_{\max} \leq 246$ GeV, then the smallest scales can be relatively low, and the production of the corresponding PGBs is consequently enhanced. This feature, i.e. the enhancement of the cross section due to the existence of low TC scales, has been first pointed out in Ref. [21], in a study of top quark production at $p\bar{p}$ colliders.

In considering the production of PGBs in e^+e^- collisions, we will concentrate in this paper on those PGBs that are electrically neutral and color singlet. There are in fact several reasons why these states are worthy of interest. First of all, the neutral and colorless PGBs are expected to be the lightest ones, since their masses do not receive contributions from the standard electroweak and strong interactions. In addition, the neutral PGBs can be singly produced in e^+e^- collisions, therefore allowing the probe of higher mass scales. Finally, the couplings of neutral PGBs to ordinary fermions and gauge bosons can be expressed in a form that is, to some extent, model independent [9]. This feature is particularly interesting, since no completely realistic TC model has been constructed so far. All the model dependence of the neutral PGB couplings to ordinary particles, fermions and gauge bosons, is explicitly included in the values of the relevant energy scales of the theory (the pseudoscalar decay constants of technipions), in the dimension of the TC gauge group, and in few model dependent couplings, which, however, are typically expected to be of order one. Thus, we are able to explore quite

general predictions of the theory for the various production and decay rates.

Nevertheless, the precise values of cross sections, for PGB production, still depend on the details of the specific model. For this reason, in discussing our results, we have allowed a large range of variability for the PGB masses and considered different values of couplings. In the lack of a completely satisfactory TC model, we will not go, in this paper, in the details of the several theoretical proposals. Our main intent is to show that the PGBs of WTC theories are expected to be produced, in presently planned experiments, for a reasonable range of model parameters, so that they are worth of an experimental research.

For illustrative purposes, we have considered in this paper a simple model of WTC, namely the multiscale TC model proposed by Lane and Ramana (LR) in Ref. [17]. The three neutral PGBs, entering in this model, are coupled with different strengths to the ordinary particles. Therefore, the analysis of this model will allow us to investigate different possible scenarios. In addition, in order to compare the WTC predictions with those of traditional, single scale, TC models, we will also consider in this paper the popular, one family, TC model proposed by Farhi and Susskind (FS) in Ref. [18].

Our results indicate that, at the LEP II experiment, the main contribution to the cross section of neutral PGB production is expected to come from the $e^+e^- \to P\gamma$ channel. In this channel, by taking into account the experimental cuts and reconstruction efficiencies, we find that several tenths of PGBs can be produced per year, assuming an integrated luminosity of 500 pb^{-1}. Possibly, a smaller PGB production can be also observed in the $e^+e^- \to Pe^+e^-$ channel. As far as the decay modes of these particles are concerned, we find that the predictions of WTC theories can be significantly different from those obtained in traditional TC models. In particular, due to the typical large values of PGB masses, a large fraction of PGB decays can also occur in the $P \to \gamma\gamma$ channel, besides the "traditional" decays into a gluon or a bottom quark pair. We then show that, at LEP II, the experimental signature of WTC events is, in most of these channels, quite distinctive, thus allowing the Standard Model background to be reduced to a negligible level.

At a 500 GeV NLC experiment, the production of neutral PGBs, predicted in WTC models, is significantly larger, and it is estimated to be of the order of 10^3 events per year, by assuming an integrated luminosity of 10^4 pb^{-1}. This production is expected to occur mainly into the $e^+e^- \to P\gamma$, $e^+e^- \to PZ^0$ and $e^+e^- \to Pe^+e^-$ channels. Instead, we find that, within the framework of traditional TC models, no PGBs are typically predicted to be observed, both at LEP II and the NLC experiment.

In the rest of this paper we will discuss our results in more detail. The LR model of WTC will be briefly reviewed in Section 2, and the masses of the lightest neutral PGBs in this model will be also estimated. In Section 3 we will discuss the general form of the neutral PGB couplings to ordinary particles. The values of the model dependent constants, entering in these couplings, will be computed in the particular case of the LR model. In Section 4, we will consider the expected decay modes of PGBs and give the results for the various production cross sections. Finally, in Section 5, we will present our conclusions.

2. The LR model of WTC

So far, a completely realistic and self-consistent TC model has not yet been constructed. In particular, the LR model we are going to discuss presents ETC gauge anomalies and predicts a too much large number of ordinary quarks and leptons. However, the model reproduces the major aspects of a typical, "quasi-realistic" model of WTC, by including several species of technifermions, several scales of technifermion chiral symmetry breaking, and $SU(2)$ isospin breaking, that accounts for the up-down mass splittings of ordinary fermions. In addition, the model is simple enough, and allows for a detailed estimates of technifermion and technipion masses. All these features turn out to be important for our purposes. In this section, we will review those aspects of the LR model that are relevant for this paper, and we refer the interested reader to Ref. [17] for more details. In addition, we will compute the values of neutral PGBs masses in this model, to be used in our subsequent phenomenological analysis.

The LR model is based on the ETC gauge group:

$$SU(N_{ETC})_1 \otimes SU(N_{ETC})_2 \tag{1}$$

where $N_{ETC} = N_{TC} + N_C + N_L$. N_{TC} represents the number of technicolors, N_C the number of ordinary colors and N_L the number of fermion flavours. The number of colors is fixed to the physical value, $N_C = 3$, while the number of technicolors, N_{TC}, and the number of flavours, N_L, are chosen to be the minimal ones to guarantee the walking of TC coupling constant. In Ref. [17], they find that this condition corresponds to $N_{TC} = N_L = 6$, and we will assume these values throughout this paper.

The dynamical symmetry breaking of the ETC group proceeds through two different steps. A first breaking occurs at the scale M_A, when the group $SU(N_{ETC})_1 \otimes SU(N_{ETC})_2$ is broken down to the diagonal subgroup $SU(N_{ETC})_{1+2}$. At a lower scale, M_V, a further breaking occurs, and the residual gauge symmetry becomes $\mathcal{G} = SU(N_{TC}) \otimes SU(3)_C \otimes SU(N_L)$. The scale M_V and M_A are estimated to be of the order of $M_V \simeq 100$ TeV and $M_A \simeq 400$ TeV.

All technifermions and ordinary fermions in the model can be classified according to the corresponding representations of the gauge group $\mathcal{G}$ to which they belong. In particular, the model contains three different species of technifermions. One doublet of color-singlet technifermions,

$$\Psi = (\Psi_U, \Psi_D) \tag{2}$$

belonging to the antisymmetric second-rank tensorial representation of the TC gauge group; one doublet of color-triplet techniquarks,

$$Q_c = (U_c, D_c) \tag{3}$$

with $c = 1, 2, 3$; and N_L doublets of color-singlet technileptons,

$$L_l = (N_l, E_l) \tag{4}$$

Table 1
Values (in GeV) of the TC scales, Λ_i, and decay constants, F_i, in the LR model, for the two sets, A and B, of model parameters

	Λ_Ψ	Λ_Q	Λ_L	F_Ψ	F_Q	F_L
A	428	83	82	231	29	28
B	876	177	172	212	43	41

with $l = 1, \ldots, N_L$. Both Q and L transform as the fundamental representation of TC gauge group $SU(N_{TC})$.

As far as the ordinary fermions are concerned, their number in the LR model is unrealistically large. With $N_L = 6$, the model contains 6 doublets of quarks, one doublets of antiquarks and $N_L\,(N_L - 1)\,/\,2 = 15$ doublets of ordinary leptons. Clearly, in order to consider the model predictions for physical processes with ordinary fermions entering in the initial and final states, we will be forced to introduce, in this respect, some approximations. However, we postpone this discussion to the last section.

The LR model of WTC is an example of multiscale TC model. Since the technifermions Ψ and Q, L belong to inequivalent representations of the TC group, they are associated to different scales (Λ_i) of TC chiral symmetry breaking [20]. Consequently, three different values of technifermion decay constants (F_i) are also expected to occur. They are constrained by the condition:

$$F_\pi \equiv \sqrt{F_\Psi^2 + 3\,F_Q^2 + N_L\,F_L^2} = 246 \text{ GeV} \tag{5}$$

that guarantees the correct physical values are assigned to the $W^\pm$ and Z^0 boson masses.

In Ref. [17], the values of F_i and Λ_i are computed by scaling the ratio Λ_i/F_i from the QCD ratio Λ_{QCD}/f_π. Two possible scaling rules have been considered, that differently take into account the dependence on the dimensionalities d_i of the $SU(N_{TC})$ technifermion representations. The first rule (A) assumes that F_i scales like $\Lambda_i\sqrt{d_i}$ (according to an expansion in $1/d_i$), while the second rule (B) assumes that $F_i\,/\,\Lambda_i$ is independent on d_i. In this way, two different sets of model parameters are obtained. The corresponding values of TC scales and decay constants are shown in Table 1. Note that a small splitting between the two lowest scales, Λ_Q and Λ_L, occurs, due to the weak effects of QCD color interactions at the TC scale.

In both sets of parameters, A and B of Table 1, the decay constant F_Ψ turns out to be quite close to the electroweak symmetry breaking scale, $F_\pi = 246$ GeV. Eq. (5) then implies that the other two scales, in the model, must be very low, of the order of few tenths of GeV. The existence of such low scales is expected to be a general feature of multiscale WTC models.

When we neglect the ETC interactions, we find that technifermions of the LR model have a large chiral flavour symmetry group:

$$[SU(2)_L \otimes SU(2)_R]_\Psi \otimes [SU(2N_L + 6)_L \otimes SU(2N_L + 6)_R]_{Q,L} \tag{6}$$

By effect of TC interactions, these chiral symmetries are spontaneously broken to the corresponding vector subgroup, and the symmetry breakdown produces $3+(2N_L+6)^2-1=326$ Goldstone bosons. Three of these particles become the longitudinal components of the $W^{\pm}$ and Z^0 bosons. The remaining 323 states represent true PGBs, that acquire mass mainly from the ETC interactions.

The large scale hierarchy in the model (see Table 1) implies that the three would-be Goldstone bosons are mainly constituted by the technifermions Ψ. Precisely, by denoting with α_Ψ^2, α_Q^2 and α_L^2 the Ψ-, Q- and L-content of the absorbed Goldstone bosons, we have:

$$\alpha_\Psi = \frac{F_\Psi}{F_\pi}, \quad \alpha_Q = \frac{\sqrt{3}\,F_Q}{F_\pi}, \quad \alpha_L = \frac{\sqrt{N_L}\,F_L}{F_\pi} \tag{7}$$

with $F_\pi = 246$ GeV (Eq. (5)). Using the values of decay constants given in Table 1, we then find that the techniquark and technilepton content of the absorbed technipions is approximately of the order of $\alpha_Q^2 + \alpha_L^2 \simeq 10 - 25\%$.

In the following, in order to simplify our analysis, we will neglect this mixing, and we will assume that the three absorbed technipions are only constituted by the technifermions Ψ, i.e. $\alpha_\Psi \simeq 1$. In this limit, the true PGBs, observed in the spectrum, are those particles only constituted by the Q and L technifermions, i.e. the states generated by the dynamical breakdown of the $SU(2N_L+6)_L \otimes SU(2N_L+6)_R$ chiral symmetry.

Three of the physical PGBs, in the model, are electrically neutral and belong to a singlet of the $SU(3)$ color group and to a singlet of the $SU(N_L)$ flavour group. The corresponding fields are proportional to the following linear combinations:

$$\begin{aligned} P_Q^3 &\sim \overline{U}_c\,\gamma^5\,U_c - \overline{D}_c\,\gamma^5\,D_c \\ P_L^3 &\sim \overline{N}_l\,\gamma^5\,N_l - \overline{E}_l\,\gamma^5\,E_l \\ P^0 &\sim N_L\,(\overline{U}_c\,\gamma^5\,U_c + \overline{D}_c\,\gamma^5\,D_c) - N_C\,(\overline{N}_l\,\gamma^5\,N_l + \overline{E}_l\,\gamma^5\,E_l) \end{aligned} \tag{8}$$

where repeated color ($c = 1,2,3$) and flavour ($l = 1,\ldots,N_L$) indexes are summed over. These PGBs are the particles we are interested in. By carrying neither color nor electric charge, they represent the lightest states of the PGB mass spectrum, and they can be produced with a larger probability in the e^+e^- collision experiments.

In order to consider these particles in our phenomenological analysis, we now estimate the size of their masses. The neutral states of Eq. (8) can only receive mass from the ETC interactions, which explicitly break technifermion chiral symmetries. We can parameterize the ETC symmetry breaking interactions in terms of an effective Hamiltonian, containing the ETC generated Q and L technifermion masses:

$$H_{ETC} = m_U\,\overline{U}U + m_D\,\overline{D}D + m_N\,\overline{N}N + m_E\,\overline{E}E \tag{9}$$

Then, at the first order in the symmetry breaking Hamiltonian, the PGB mass matrix is given by the Dashen formula [24]:

$$\left(M_P^2\right)_{ab} = \frac{1}{F_P^2}\,\langle 0 \mid \left[Q_5^a, \left[Q_5^b, H_{ETC}(0)\right]\right] \mid 0\rangle \tag{10}$$

Table 2
Values of the technifermion condensates (in unit of $(\mathrm{GeV})^3$) and masses (in GeV), evaluated at the TC scale $\Lambda_Q \simeq \Lambda_L$, in the LR model, for the two sets, A and B, of model parameters

	$\langle \bar{Q}Q \rangle$	$\langle \bar{L}L \rangle$	m_U	m_D	m_N	m_E
A	$(69)^3$	$(66)^3$	136	22	61	13
B	$(114)^3$	$(109)^3$	92	14	43	9

where F_P is the decay constant ($F_P = F_Q \simeq F_L$), H_{ETC} is the symmetry breaking Hamiltonian (Eq. (9)) and Q_5^a are the axial charges associated with the flavour chiral symmetry group.

The explicit evaluation of the commutators in the Dashen formula is cumbersome but straightforward. One then finds that the mass matrix of the three neutral PGBs is not diagonal, since the mass splittings, $(m_U - m_D)$ and $(m_N - m_E)$, give raise to a mixing among the states of Eq. (8). In a first approximation, we can neglect this mixing, by simply neglecting the off-diagonal elements of the PGB mass matrix. We then find that the masses of the three light neutral PGBs in the model are given by the expressions:

$$M_{3Q}^2 F_Q^2 = (m_U + m_D)_{\Lambda_Q} \langle \bar{Q}Q \rangle_{\Lambda_Q} , \qquad M_{3L}^2 F_Q^2 = (m_N + m_E)_{\Lambda_L} \langle \bar{L}L \rangle_{\Lambda_L} ,$$

$$M_0^2 F_Q^2 = \left(\frac{N_L}{N_L + N_C} \right) (m_U + m_D)_{\Lambda_Q} \langle \bar{Q}Q \rangle_{\Lambda_Q} + \left(\frac{N_C}{N_L + N_C} \right) (m_N + m_E)_{\Lambda_L} \langle \bar{L}L \rangle_{\Lambda_L} \tag{11}$$

where $\langle \bar{Q}Q \rangle$ and $\langle \bar{L}L \rangle$ are the techniquark and technilepton condensates. The values of these condensates and the values of the technifermion masses have been evaluated in Ref. [17], and they are presented in Table 2 for the two sets, A and B, of model parameters. By substituting these values in Eq. (11), we then obtain (in GeV):

$$\begin{aligned} &(A) \quad M_{3Q} = 247 , \quad M_{3L} = 166 , \quad M_0 = 223 \\ &(B) \quad M_{3Q} = 293 , \quad M_{3L} = 200 , \quad M_0 = 266 \end{aligned} \tag{12}$$

This calculation can be now repeated by correctly taking into account the mixing among the three PGBs. In this case, by denoting with M_{P1}, M_{P2} and M_{P3} the eigenvalues of the PGB mass matrix, we find (in GeV):

$$\begin{aligned} &(A) \quad M_{P1} = 304 , \quad M_{P2} = 118 , \quad M_{P3} = 173 \\ &(B) \quad M_{P1} = 362 , \quad M_{P2} = 137 , \quad M_{P3} = 205 \end{aligned} \tag{13}$$

Thus, the masses of the three neutral PGBs, in the LR model, are in the range between 100 and 350 GeV. The main source of uncertainty in this estimate comes from the scaling from QCD of the PGB decay constants and technifermion condensates. For this reason, the results of Eqs. (12) and (13) must be considered as purely indicative. However, it is also reasonable to assume that they correctly represent the typical order of magnitude of the lightest PGB masses in the framework of a general multiscale WTC models.

3. The couplings of neutral PGBs to ordinary particles

In TC/ETC theories, the couplings of the neutral PGBs to ordinary fermions and gauge bosons are, to some extent, model independent. All the model dependence of these couplings is included in the values of the relevant energy scales of the theory, the pseudoscalar decay constants of technipions, in the dimension of the TC gauge group, N_{TC}, and in two classes of constants which, however, are typically expected to be of order one. In this section, we will write down the general form of these couplings and we will compute the values of the model dependent constants in the particular case of the LR model.

3.1. Couplings of neutral PGBs to gauge bosons

Let us first define the couplings of neutral PGBs with two arbitrary gauge bosons of the Standard Model.

At the energy scales smaller than the typical TC scale, Λ_{TC}, the couplings between a PGB P and two gauge bosons, B_1 and B_2, are controlled by the ABJ anomaly [25]. By adopting a convenient parameterization, these couplings can be written in the form [9]:

$$\frac{1}{(1+\delta_{B_1B_2})}\left(\frac{\alpha\, d_{TC}\, A_{PB_1B_2}}{\pi F_P\sqrt{n/2}}\right) P\,\epsilon_{\lambda\mu\nu\rho}\,(\partial^\lambda B_1^\mu)\,(\partial^\nu B_2^\rho) \tag{14}$$

where P, B_1^μ and B_2^μ represent the field operators of the PGB and the two gauge bosons B_1 and B_2 respectively. F_P is the PGB decay constant, n is the dimension of the chiral flavour symmetry group and d_{TC} is the dimensionality of the TC representation to which the technifermions T, constituting the PGB P, belong. In the LR model, for instance, when we consider the techniquark and technilepton sector, we have $n = 2(N_L + 3)$ and $d_{TC} = N_{TC}$. Since technifermions entering in the fundamental representation of the group $SU(N_{TC})$ is a very usual condition in TC models, in the following we will always consider the case $d_{TC} = N_{TC}$. We also define α, in Eq. (14), to be $e^2/4\pi$ if B_1 and B_2 are electroweak gauge bosons, and equal to the strong coupling constant, α_s, if B_1 and B_2 are QCD gluons.

The coupling $A_{PB_1B_2}$, in Eq. (14), is a group theoretical factor. It is defined by the relation:

$$4\pi\alpha\sqrt{2/n}\,A_{PB_1B_2} = g_1 g_2\,\mathrm{Tr}\left[Q_P\left(\{Q_V^1, Q_V^2\} + \{Q_A^1, Q_A^2\}\right)\right] \tag{15}$$

where g_i is the gauge coupling of the boson B_i and $Q_{V,A}^i$ are the corresponding vector and axial charges. Q_P is the axial charge of the PGB P. The factor $\sqrt{2/n}$, entering in Eq. (15), approximately takes into account the dependence of the anomalous couplings on the dimension of the flavour group, in such a way that the coupling $A_{PB_1B_2}$ is expected to be a constant of order one, independently on the particular TC model one is considering [9].

Table 3
Expressions and numerical values of the constants $A_{PB_1B_2}$ in the FS and LR models. The symbols s_W, c_W and t_W represent the sine, cosine and tangent of the Weinberg angle respectively, and the numerical values have been obtained by using $s_W^2 = 0.23$

FS	A_{PZZ}		$A_{PZ\gamma}$		$A_{P\gamma\gamma}$		$A_{Pg^ag^a}$	
P^0	$-\frac{4}{3\sqrt{3}}t_W^2$	−0.23	$\frac{4}{3\sqrt{3}}t_W$	0.42	$-\frac{4}{3\sqrt{3}}$	−0.77	$\frac{1}{\sqrt{3}}$	0.58
P^3	$-\frac{4}{\sqrt{3}}\frac{(1-2s_W^2)}{2c_W^2}$	−0.81	$\frac{4}{\sqrt{3}}\frac{(1-4s_W^2)}{4s_Wc_W}$	0.11	$\frac{4}{\sqrt{3}}$	2.31	0	0.00
LR	A_{PZZ}		$A_{PZ\gamma}$		$A_{P\gamma\gamma}$		$A_{Pg^ag^a}$	
P^0	$-\frac{4\sqrt{2}}{3}t_W^2$	−0.56	$\frac{4\sqrt{2}}{3}t_W$	1.03	$-\frac{4\sqrt{2}}{3}$	−1.89	$\sqrt{2}$	1.41
P_Q^3	$-\sqrt{3}\frac{(1-2s_W^2)}{2c_W^2}$	−0.61	$\sqrt{3}\frac{(1-4s_W^2)}{4s_Wc_W}$	0.08	$\sqrt{3}$	1.73	0	0.00
P_L^3	$3\sqrt{6}\frac{(1-2s_W^2)}{2c_W^2}$	2.58	$-3\sqrt{6}\frac{(1-4s_W^2)}{4s_Wc_W}$	−0.35	$-3\sqrt{6}$	−7.35	0	0.00

It is useful to verify such approximate model independence by considering some particular cases. In the $\pi^0 \to 2\gamma$ decay of QCD, we have $d_{TC} = 3$ (in this case, this is the number of ordinary colors), $n = 2$ (the dimension of the flavour symmetry group) and $A_{\pi^0\gamma\gamma} = 1/3$.

In the traditional, one family, TC model, introduced by Farhi and Susskind in Ref. [18], there exist one doublet of color-triplet techniquark, $Q_c = (U_c, D_c)$, and one doublet of color-singlet technileptons, $L = (N, E)$. In this model, the spontaneous breakdown of the $SU(8)_L \otimes SU(8)_R$ chiral symmetry of technifermions results in 63 Goldstone bosons, two of which, P^0 and P^3, are neutral and colorless:

$$\begin{aligned} P^0 &\sim (\overline{U}_c\gamma^5 U_c + \overline{D}_c\gamma^5 D_c) - 3(\overline{N}\gamma^5 N + \overline{E}\gamma^5 E) \\ P^3 &\sim (\overline{U}_c\gamma^5 U_c - \overline{D}_c\gamma^5 D_c) - 3(\overline{N}\gamma^5 N - \overline{E}\gamma^5 E) \end{aligned} \tag{16}$$

They belong to an isospin singlet and triplet respectively, and they are expected to be the lightest PGB states contained in the model. The values of the corresponding model dependent constants, $A_{PB_1B_2}$, for B_1B_2 equal to ZZ, $Z\gamma$, $\gamma\gamma$ and a gluon pair, g^ag^b, are shown in the upper side of Table 3. In this table, together with the analytical expressions, we also give the corresponding numerical values, obtained by using $s_W^2 = 0.23$, where s_W is the sine of the Weinberg angle. From Table 3, we see that all these constants are approximately of order one.

Clearly, some particular deviations from unity can always occur. For example, the coupling $A_{P^3Z\gamma}$, of the PGB P^3, turns out to be quite small, being proportional to the small combination $(1-4s_W^2)$. As observed in Refs. [7,8], for all the PGBs belonging to a triplet representation of the isospin group, this proportionality is a general consequence

of the underlying custodial $SU(2)$ symmetry. The same symmetry also produces the vanishing of the P^0 and P^3 couplings to a W^+W^- boson pair and the vanishing of the coupling between the isovector P^3 and a QCD gluon pair.

In the lower side of Table 3, we give the values of the couplings $A_{PB_1B_2}$ for the three light neutral PGBs of the LR model. Note how the structure of these coefficients is fixed by the custodial $SU(2)$ symmetry. The couplings of the PGBs P_Q^3 and P_L^3, of the LR model, are proportional to those of the PGB P^3 in the FS model, and similarly for the couplings of the two isoscalar P^0's. Moreover, we find that, also in LR model, all these couplings are of the order of one, thus supporting the statement of their approximate independence on the particular choice of the TC model.

3.2. *High energy corrections to anomalous couplings*

The form of the anomalous coupling, considered in Eq. (14), is expected to be exactly valid only in the limit in which the energy scales and the masses of the particles, involved in the process, are smaller than the typical TC scale, Λ_{TC}. In WTC theories, however, the masses of the PGBs are typically of the order of Λ_{TC}. Moreover, we are going to consider in this paper physical processes occurring at the energy scales of the LEP II and NLC experiments, namely 200 and 500 GeV respectively. Even these scales are both of the order, or even larger, than Λ_{TC}. Thus, in computing the corresponding cross sections, the use of the anomalous couplings of Eq. (14) might be questionable.

The fact that the couplings of Eq. (14) lose their validity in the high energy limit is also indicated by the following observation. Let us consider any process in which a virtual gauge boson, B_1, is produced in the s-channel, and it is coupled, via the anomaly, to a PGB and a second gauge boson, B_2. An example of this process is $e^+e^- \to \gamma^* \to P\gamma$. Since the couplings of Eq. (14) turn out to be inversely proportional to the pseudoscalar decay constant F_P, one can argue, from simple dimensional arguments, that, in the high energy limit, the corresponding cross sections must behave like a constant. Indeed, this is just what we will find, after an explicit calculation, in Section 4 (see Eq. (24) below). The same problem arises in QCD, if one considers, in the high energy limit, the π^0 production in the $e^+e^- \to \pi^0\gamma$ channel. Thus, at high energies, the anomalous couplings of Eq. (14) violate the unitarity of the theory.

By considering parity and Lorentz invariance, it is easy to realize that the general form of the couplings between a PGB and two vector gauge bosons is still given by Eq. (14) times an invariant form factor.

In QCD, or in a strongly interacting TC theory, this "anomalous" form factor can be only evaluated with a full non-perturbative calculation of the two triangle diagrams, that, in the low energy limit, originate the anomaly. In these diagrams, the quark or technifermion lines, coupled in a vertex to a pseudoscalar source, give rise, by effect of their mutual strong interactions, to the propagation of the PGB field.

In the lack of a non-perturbative calculation, we try to estimate the high energy behaviour of the triangle diagrams in the context of a phenomenological model. We have considered a simple version of the linear σ model, containing one charged fermion

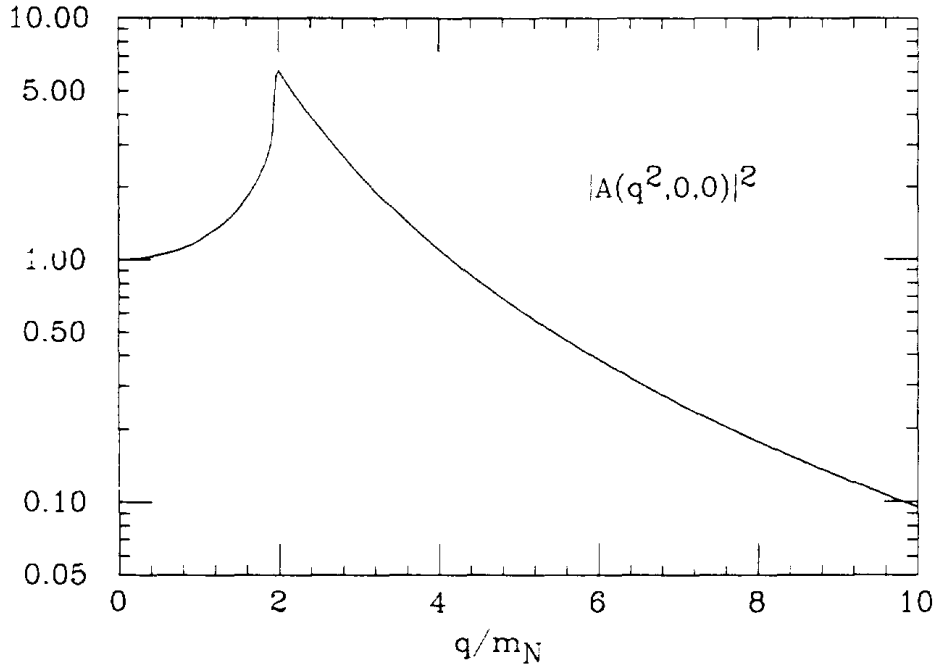

Fig. 1. The form factor $|A\left(q^2, k_1^2, k_2^2\right)|^2$ as a function of the dimensionless variable $\sqrt{q^2/m_N^2}$, for $k_1^2 = k_2^2 = 0$.

field (the proton), one pseudoscalar field (the neutral pion) and the scalar σ field. In this model, the effective coupling between the pion and two vector gauge boson can be easily computed, and the result for the anomalous form factor has the form:

$$A\left(q^2, k_1^2, k_2^2\right) = \int_0^1 dx \int_0^1 dy \int_0^1 dz \, \frac{2\,\delta(1-x-y-z)}{\left[1 - \frac{q^2}{m_N^2}\,xy - \frac{k_1^2}{m_N^2}\,xz - \frac{k_2^2}{m_N^2}\,yz - i\epsilon\right]} \tag{17}$$

where q, k_1 and k_2 are the four-momenta of the PGB and the two gauge bosons, and m_N is the nucleon mass. The form factor is properly normalized at zero momenta, $A(0,0,0) = 1$.

In Fig. 1, $|A\left(q^2, k_1^2, k_2^2\right)|^2$ is shown as a function of the dimensionless variable $\sqrt{q^2/m_N^2}$, for $k_1^2 = k_2^2 = 0$. This choice corresponds, for instance, to the $P \to 2\gamma$ decay, with $q^2 = M_P^2$, or to the $e^+e^- \to P\gamma$ process, when q^2 is the energy square in the center of mass and $M_P^2 = 0$.

Fig. 1 shows that, in the region of small q^2, the form factor $|A\left(q^2, 0, 0\right)|^2$ is an increasing function of the momenta, until it reaches a peak in correspondence of $q^2 = 4m_N^2$. For $q^2 \geq 4m_N^2$, the form factor acquires a non zero imaginary part, that would correspond, according to the Cutkosky rule, to the possible creation of a real nucleon pair in the $P \to NN$ channel. Above this threshold, the form factor starts to decrease for increasing q^2, thus correcting the bad asymptotic behaviour of the corresponding cross sections.

Let us now discuss these results in the framework of QCD. In QCD, the anomalous $\pi^0 \to 2\gamma$ decay rate, calculated in the limit $m_\pi = 0$, is in agreement with the experimental value within less than a few per cent of accuracy. In this case, the anomalous

form factor, as given from Eq. (17), would only introduce a correction of the order of 0.3%, thus strongly supporting the validity of the $m_\pi = 0$ approximation.

A priori, one could expect that very large corrections to the couplings of Eq. (14) would be found in the case of the $\eta \to 2\gamma$ and $\eta' \to 2\gamma$ decays, since the masses of these mesons are of order of two or three times Λ_{QCD}. However, the evaluation of the anomalous form factor, in the linear σ model, indicates that this is not the case. For a PGB mass equal to the η' mass, we find that this correction is of the order of 20%. On the other hand, the $\eta \to 2\gamma$ and $\eta' \to 2\gamma$ decay rates, when computed in the limit of zero meson masses, are consistent, with the corresponding experimental values, within approximately a factor of 1.5, with a large theoretical uncertainty coming, in this case, from the unknown value of the $\eta - \eta'$ mixing angle. This uncertainty is too large to draw any definite conclusion. However, the estimate of the anomalous form factor, obtained in the linear σ model, seems consistent with the experimental data.

These arguments suggest that the high energy corrections, to the anomalous couplings of Eq. (14), only become relevant, in QCD, when the typical energy scale in the process is of the order of several times the nucleon mass. In particular, the anomalous form factor of Fig. 1, is found to be still of the order of one when the energy scale is equal to $4\,m_N$, and it is reduced by one order of magnitude only when the energy becomes of the order of $\sim 10\,m_N$.

Let us now apply these results in the framework of TC theories. The relevant energy scale, entering in the expression of the form factor, is expected to be the techninucleon mass (or, possibly, the mass of the lightest technihadron coupled in pair to the technipion). In a QCD-like TC model, this mass can be simply estimated by scaling from QCD and using large-N arguments. One then finds the result:

$$M_{T-Nucleon} = \left(\frac{\Lambda_{QCD}}{\Lambda_{TC}}\right)\left(\frac{N_{TC}}{3}\right) m_{Nucleon} \tag{18}$$

For a WTC model, the simple scaling from QCD is not expected to be accurate. However, by not having a better prescription, we can only rely on this approximation. Thus, when applied for example to the LR model, Eq. (18) indicates that, in the technilepton and techniquark sector, the techninucleon masses are in the range between 400 and 800 GeV, depending on the set of parameters, A or B in Table 1, one is considering.

In practice, the precise values of these masses are not relevant for our purposes. We just observe that, if the technihadrons have masses in the range of several hundred GeV, then the corrections introduced by the anomalous form factor to the couplings of Eq. (14) are likely to be of the order of only $10 - 20\%$, either for PGB masses of the order of Λ_{TC}, or for processes occurring at the 500 GeV energy of the NLC experiment. On the other hand, these corrections are likely to be of the same order of magnitude of the theoretical uncertainties affecting the calculation of the form factor itself. For these reasons, we will not attempt to take them into account. We just conclude that, in all the processes we are going to consider in this paper, the interactions between PGBs and ordinary gauge bosons are expected to be described, reasonably well, by the couplings of Eq. (14).

3.3. Couplings of neutral PGBs to ordinary fermions

The PGBs of TC theories are also coupled to the ordinary fermions by the ETC interactions. In models of TC, the ETC interactions are introduced in order to explicitly break the fermion chiral symmetries, and to generate the ordinary fermion and technifermion masses [4,5]. In the low energy limit, with respect to Λ_{ETC}, the ETC interactions can be described in terms of an effective Lagrangian, which contains four-fermion couplings between ordinary fermions and technifermions. These couplings also describe the interactions between the PGBs and the ordinary fermion pairs.

The most general form of the ETC effective Lagrangian has been discussed in Ref. [5]. It is possible to show, starting from this general case, that the coupling between a neutral PGB P and an ordinary fermion pair, $\bar{f}f$, is expected to be proportional to the fermion mass m_f, and to the inverse of the pseudoscalar decay constant F_P, $g_{Pff} \sim m_f/F_P$ [1].

Starting from this result, and following Ref. [9], we then write the coupling between a neutral PGB P and a fermion pair $\bar{f}f$ in terms of a second class of model dependent constants, B_{Pff}, in the form:

$$-B_{Pff}\left(\frac{m_f}{F_P\sqrt{n/2}}\right)P\,(\bar{f}\,i\gamma^5 f) \tag{19}$$

The precise values of the constants B_{Pff} depend on the structure of the ETC gauge group and the fermion and technifermion contents of the ETC representations. However, with the definition of Eq. (19), all these constants are typically expected to be of order one, and we refer the reader to Ref. [9] for some specific examples.

In this paper, we will not go in further details on this point. By having defined the general form of the PGB couplings to both ordinary gauge bosons and fermions, Eqs. (14) and (19), we now proceed to compute the various rates of PGB production and decay in the e^+e^- collision experiments.

4. The production and decay of neutral PGBs in e^+e^- collisions

In the analysis of the LR model, performed in Section 2, we found that the masses of the three lightest PGBs are approximately in the range between 100 and 350 GeV (see Eqs. (12) and (13)). One can argue that this is a quite general result. In WTC models, the masses of those light PGBs, that are only generated by the ETC interactions, are generally estimated to be of the order of the relevant TC scale, Λ_{TC}. In models with a single scale of dynamical symmetry breaking, Λ_{TC} is roughly of the order of 500 GeV. In multiscale models, where a few low energy scales can appear, it is unlikely that these scales, and, hence, the PGB masses, can be smaller than 100 GeV. For this reason, in

[1] This is the analog of the Goldberger and Treiman relation in QCD, which describes the effective coupling between the pion and a nucleon pair.

the rest of this paper, by considering the results of Eqs. (12) and (13), we will only allow the neutral PGB masses to vary in the range between 100 and 350 GeV.

From a phenomenological point of view, it follows that, in order to discuss the PGB production in e^+e^- collision, it is reasonable to assume that the PGBs of WTC are too heavy to be produced from on-shell Z^0 decays, e.g. at the LEP I or SLC experiments. Thus, we will only consider in this paper the PGB production at the two presently planned high energy e^+e^- colliders, namely LEP II and NLC. For these experiments, we will assume the energy in the center of mass to be equal to 200 and 500 GeV, and the integrated luminosity per year to be equal to $5 \cdot 10^2$ and 10^4 pb^{-1} respectively.

The several cross sections and decay rates, relevant for the PGB production in e^+e^- collisions, will be computed in the framework of a generic TC/ETC model. The dependence of the results on the particular model is introduced by the value of the PGB decay constant, F_P, the number of technicolors, N_{TC}, the dimension n of the flavour symmetry group, and the PGB couplings, $A_{PB_1B_2}$ and B_{Pff}. From Eqs. (14) and (19), it is clear that the two model dependent quantities, F_P and n, will always appear through the combination $F_P\sqrt{n/2}$. In traditional single-scale TC models this combination is constrained to be equal to the electroweak scale, $F_\pi = 246$ GeV. Thus, as far as the traditional TC models are concerned, our predictions are actually independent on the value of the specific TC scale.

In presenting the numerical results for WTC models we will consider, in particular, the predictions obtained in the framework of the LR model discussed in Section 2. In this case, in order to simplify the discussion, we will identify the mass eigenstates, in the light PGB sector, with the three weak isospin eigenstates defined in Eq. (8), namely the PGBs P^0, P_Q^3 and P_L^3. Thus, as far as these PGBs are concerned, we will neglect the mixing introduced in the model by the explicit isospin symmetry breaking. With this assumption, the values of the couplings $A_{PB_1B_2}$, between the PGBs and the ordinary gauge bosons, are those given in Table 3. To be specific, we will only consider, in the following, the values of technipion decay constants labelled as set A in Table 1. With the values denoted as set B, we would have obtained smaller values, of the order of 50%, for the corresponding cross sections (this ratio scales approximately as $(F^A/F^B)^2$).

As already observed in Section 2, one of the unrealistic aspects of the LR model is the flavour content of ordinary fermions. With $N_L = 6$, the model predicts the existence of six doublets of quarks, one doublets of antiquarks and $N_L(N_L-1)/2 = 15$ doublets of ordinary leptons. On the other hand, the choice of a smaller value of N_L (e.g. the more "realistic" choice $N_L = 3$) would not guarantee anymore the walking of the TC coupling constant and, consequently, the onset of WTC dynamics. Thus, in order to obtain sensible predictions, we will keep N_L fixed to the value $N_L = 6$, and we will simply assume that, among the whole set of ordinary fermions, there exist the three standard families of quarks and leptons observed in the experiments. Only these particles will be then considered as possible candidates in the final states. Furthermore, in presenting all our numerical results, we will allow the values of the model dependent ETC couplings, $B_{PB_1B_2}$, to vary in the range between 1/3 and 3.

4.1. The decays of PGBs in multiscale WTC models

In order to investigate the experimental signatures expected when the PGBs are produced in e^+e^- collisions, we first consider, in this section, the possible decay modes of these particles. Since, within the framework of traditional TC models, the PGB decays have been already extensively discussed in the literature (see e.g. Refs. [6] and [26]), we will concentrate here on those aspects of neutral PGB decays that are peculiar of WTC dynamics.

By being the lightest states among all the existing technihadrons, the neutral PGBs we are considering in this paper are not allowed to decay via the strong TC interactions. Thus, they can only decay either into a pair of standard gauge boson, through the anomalous couplings of Eq. (14), or into an ordinary fermion-antifermion pair, through the ETC couplings of Eq. (19). The corresponding decay widths, expressed in terms of the model dependent constants $A_{PB_1B_2}$ and B_{Pff}, are given by:

$$\Gamma(P \to B_1 B_2) = \frac{N_C}{(1+\delta_{B_1B_2})} \left(\frac{\alpha^2 A^2_{PB_1B_2} N^2_{TC}}{32\pi^3 F_P^2 (n/2)} \right) M_P^3 \, \lambda\left(1, \frac{M^2_{B_1}}{M^2_P}, \frac{M^2_{B_2}}{M^2_P}\right) \quad (20)$$

and

$$\Gamma(P \to \bar{f} f) = N_C \left(\frac{B^2_{Pff}}{8\pi F_P^2 (n/2)} \right) M_P \, m_f^2 \sqrt{1 - \frac{4m_f^2}{M_P^2}} \quad (21)$$

In these equations, N_C represents the number of colors of the two particles in the final state: $N_C = 3$ for quarks, $N_C = 8$ for gluons and $N_C = 1$ for leptons and electroweak gauge bosons. In addition, the function λ is defined as:

$$\lambda(a,b,c) \equiv a^2 + b^2 + c^2 - 2ab - 2bc - 2ac \quad (22)$$

Since the decay widths in Eqs. (20) and (21) are both proportional to $1/F_P^2$, the corresponding branching ratios turn out to be independent on the value of the specific TC scale. Thus, we find that the existence of low energy scales, in multiscale WTC models, does not affect the relative weight of the various branching ratios, with respect to the predictions of traditional TC models. The only effect of such low scales, is a net increasing of the total PGB decay widths.

In contrast, a considerable effect of WTC dynamics in PGB decays, comes from the typically large values of PGB masses. Indeed, the decay widths of PGBs into gauge boson pairs are proportional to the third power of the PGB mass, while the decay widths into ordinary fermion pairs only increase linearly with this mass. Thus, we expect that the large PGB masses, predicted in WTC models, will enhance the several $P \to B_1 B_2$ branching ratios with respect to those of the $P \to \bar{f} f$ decays.

As an example, let us consider the partial decay widths of the three light neutral PGBs of the LR model. The two isovectors, P_Q^3 and P_L^3, are not coupled to a QCD gluon pair. Thus, the gluon-gluon decay is only allowed for the PGB P^0. In this case, the relevant coupling, $A_{P^0 g^a g^a}$, is equal to $\sqrt{2}$, and one finds that, for this particle, the

decay mode into a gluon pair represents the favored channel. For instance, by assuming that the ETC coupling constants, B_{Pff}, are all equal to one, we find that the $P^0 \to gg$ branching ratio can vary between 92%, for $M_P = 100$ GeV, and 99%, for $M_P = 350$ GeV. If we consider larger values of the ETC couplings, for example $B_{Pff} = 3$, then we find that the PGB P^0 is also expected to decay in a $\bar{b}b$ pair in approximately 40% of the cases, if its mass is equal to 100 GeV. However, this probability is reduced to less than 15% for $M_P = 200$ GeV, and to approximately 5% for $M_P = 350$ GeV.

If the PGBs are not coupled to a gluon pair, as the PGBs P_Q^3 and P_L^3 of the LR model, then the preferred decay mode of these particles is expected to be into a pair of bottom quarks. For the PGB P_Q^3, for example, if the ETC constants B_{Pff} are all equal to one, the $P_Q^3 \to \bar{b}b$ branching ratio varies between 87% and 78%, as its mass increases from 100 to 350 GeV. The remaining decay modes occur mainly into a pair of $\bar{c}c$ ($\simeq 7-8\%$) or $\tau^+\tau^-$ ($\simeq 3-4\%$). However, for smaller values of the ETC couplings, and for large values of the PGB mass, a considerable fraction of the PGB decays can also occur into the anomalous channel $P \to \gamma\gamma$. For $B_{Pff} = 1/3$ and $M_P = 200$ GeV, the $P \to \gamma\gamma$ branching ratio is equal to approximately 26%. For even larger PGB masses, for example $M_P = 350$ GeV, the decay mode into a photon pair is the dominant one, with a branching ratio of approximately 50%. In this case, the fraction of $P \to \bar{b}b$ decay mode is of the order of 40%.

The decay mode into a photon pair is even more relevant for the PGB P_L^3. In this case, in fact, the corresponding coupling $A_{P_L^3\gamma\gamma}$ has a value which is significantly larger with respect to one: $A_{P_L^3\gamma\gamma} \simeq -7.35$ (see Table 3). The resulting scenario is then illustrated in Fig. 2, in which the values of the $P \to \gamma\gamma$ and $P \to \bar{b}b$ branching ratios, for the PGB P_L^3, are plotted as a function of the PGB mass. In the figure, the three values $B_{Pff} = 1/3$, 1 and 3 have been considered. By looking at Fig. 2, we find that, when B_{Pff} is equal to 1/3, the $P_L^3 \to \gamma\gamma$ channel represents the dominant decay mode of this particle, regardless of the value of its mass. The corresponding branching ratios vary between 61%, for $M_P = 100$ GeV, and 88%, for $M_P = 350$ GeV. For $B_{Pff} = 1$, the decay mode into a photon pair can still be dominant, but only for a PGB mass larger than approximately 220 GeV. Finally, for an even larger value of the ETC coupling, $B_{Pff} = 3$, the PGB P_L^3 is expected to decay mainly into a $\bar{b}b$ pair.

In conclusion, we see that, in WTC theories, the predictions for PGB decays can significantly differ from those obtained in the framework of traditional TC models. Due to the large values of masses expected in WTC theories, the $P \to \gamma\gamma$ decay can represent a large fraction of the all PGB decay modes, whereas this channel is usually strongly suppressed in traditional models. The specific values of PGB branching ratios, however, are to a large extent model dependent. They strongly depend on the values of the PGB masses and the values of the model dependent coupling constants. Nevertheless, in performing a phenomenological analysis, we can take advantage of the fact that only few relevant decay modes of these particles have to be considered, namely the decays $P \to gg$, $P \to \bar{b}b$ and $P \to \gamma\gamma$. In addition, the $P \to gg$ decay is forbidden for all the PGBs with isospin one.

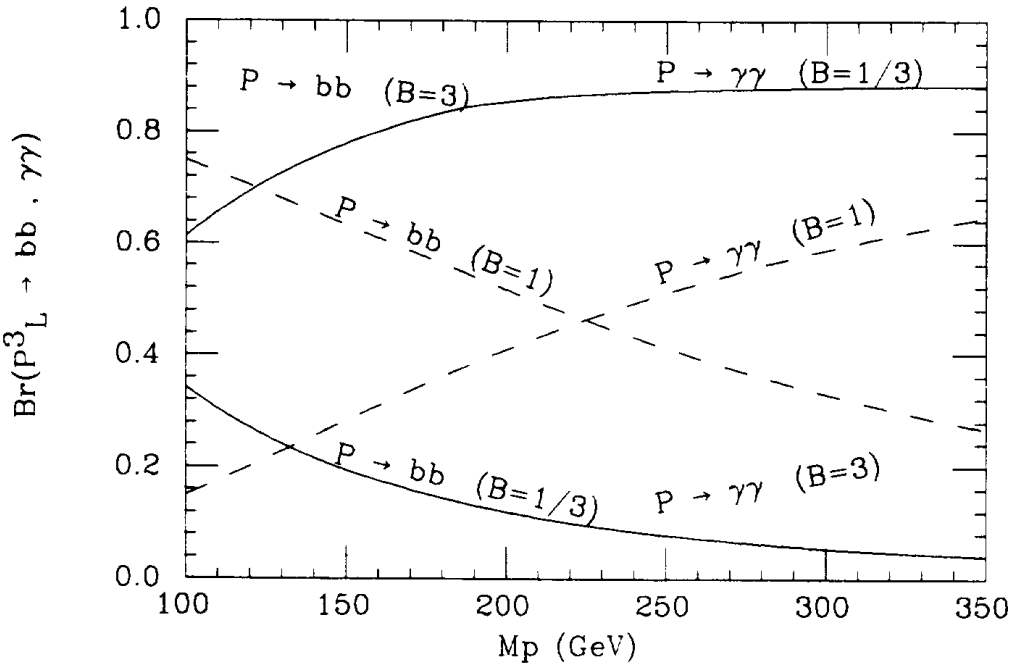

Fig. 2. The $P \to \gamma\gamma$ and $P \to \bar{b}b$ branching ratios, for the PGB P_L^3 of the LR model, as a function of the PGB mass M_P. The curves correspond to the values $B_{Pff} = 1/3$ (solid), $B_{Pff} = 1$ (dashes) and $B_{Pff} = 3$ (dots) of the ETC coupling constants.

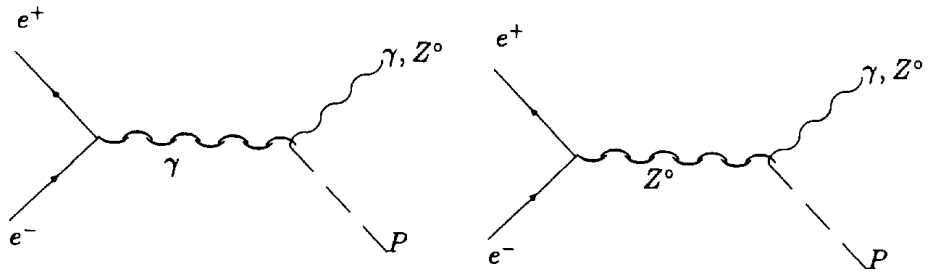

Fig. 3. Feynman diagrams relevant for the processes $e^+e^- \to P\gamma$ and $e^+e^- \to PZ^0$.

4.2. *The production of PGBs in the $e^+e^- \to P\gamma$ and $e^+e^- \to PZ^0$ channels*

We now consider the production of PGBs in e^+e^- collisions. In these experiments, the simplest channels of neutral PGB production are represented by the processes:

$$e^+e^- \to P\gamma\,, \qquad e^+e^- \to PZ^0 \tag{23}$$

At the lowest order of perturbation theory, each of these processes is described by the two Feynman diagrams of Fig. 3. Both these diagrams are only controlled by the anomalous TC couplings between the PGBs and the ordinary gauge bosons, and they do not involve the presence of the ETC interactions.

Since the lightest PGB masses are likely in the range between 100 and 350 GeV, then the $e^+e^- \to PZ^0$ channel is practically forbidden at the LEP II experiment, while

the $e^+e^- \to P\gamma$ is allowed, provided that the PGBs have masses smaller than 200 GeV. In the NLC experiment, with an energy of 500 GeV in the center of mass, both these channels are open.

The total cross section, for the processes in Eq. (23), has been computed in Ref. [8], where, however, it is only discussed in the framework of traditional TC models. In terms of the couplings $A_{PB_1B_2}$, the result has the form:

$$\sigma(e^+e^- \to PB) = \left(\frac{\alpha^3 N_{TC}^2}{24\pi^2 F_P^2 (n/2)}\right) \lambda^{3/2}(1, m_P^2, m_B^2) \times \left[A_{PB\gamma}^2 + \frac{A_{PB\gamma} A_{PBZ} (1 - 4 s_W^2)}{2 s_W c_W (1 - m_Z^2)} + \frac{A_{PBZ}^2 (1 - 4 s_W^2 + 8 s_W^4)}{8 s_W^2 c_W^2 (1 - m_Z^2)^2}\right] \tag{24}$$

where B may be a photon or a Z^0 gauge boson. In Eq. (24), $\sqrt{s}$ is the energy in the center of mass, m_P and m_B are the particle masses in units of $\sqrt{s}$, and the function λ is defined in Eq. (22). Of the three terms entering in Eq. (24), the first and the last one describe the contribution of the two diagrams of Fig. 3, while the second term represents the interference between them. Note that, as discussed in Section 3, without the introduction of the anomalous form factor, the cross section in Eq. (24), in the high energy limit, $s \to \infty$, tends to be constant.

The $\sigma(e^+e^- \to PB)$ cross section is proportional to the factor $1/F_P^2 (n/2)$. This is the origin of the enhancement of the cross section in multiscale WTC models. In the LR model, for example, the scale $F_P = F_Q \simeq F_L$ is of the order of approximately 30 GeV (see Table 1), and the number of technifermion species is $n = 2(N_L + 3) = 18$. Thus, the quantity $F_P\sqrt{n/2}$ is equal to approximately 90 GeV, and it is smaller by almost a factor of three with respect to the value $F_P\sqrt{n/2} \simeq 246$ GeV occurring in models with a single TC scale. This means that the values of the corresponding cross sections are larger by approximately one order of magnitude.

Eq. (24) can be used to compute the $\sigma(e^+e^- \to PB)$ cross section in any model of interest. In order to discuss these processes in a more quantitative way, we show in Fig. 4 the values of this cross section, in the $e^+e^- \to P\gamma$ channel, as a function of the PGB mass M_P, for the three PGBs P_L^3, P_Q^3 and P^0 of the LR model. The energy in center of mass is fixed to the LEP II value of 200 GeV. We see from the figure that the total cross section, in the case of the PGB P_L^3, is larger by approximately one order of magnitude with respect to the values obtained for the PGBs P_Q^3 and P^0. The reason of such a difference is the large value that the coupling $A_{P_L^3\gamma\gamma}$ assumes in the LR model. For this particle, we find that the values of the $\sigma(e^+e^- \to P_L^3\gamma)$ cross section, at the energy of 200 GeV, vary between 10^{-1} and 10^{-2} pb, in the range of PGB masses between 100 and 150 GeV. This corresponds, at LEP II, to a production rate of approximately 10-50 PGBs per year. Due to the strong phase space suppression, this rate becomes then negligible when the PGB mass is larger than 150 GeV.

On the other hand, when we consider the PGBs P_Q^3 and P^0, we find from Fig. 4 that the number of $e^+e^- \to P\gamma$ events per year is expected to be only of the order of few units, even for PGB masses of approximately 100 GeV. For the two PGBs, P_Q^3 and P^0,

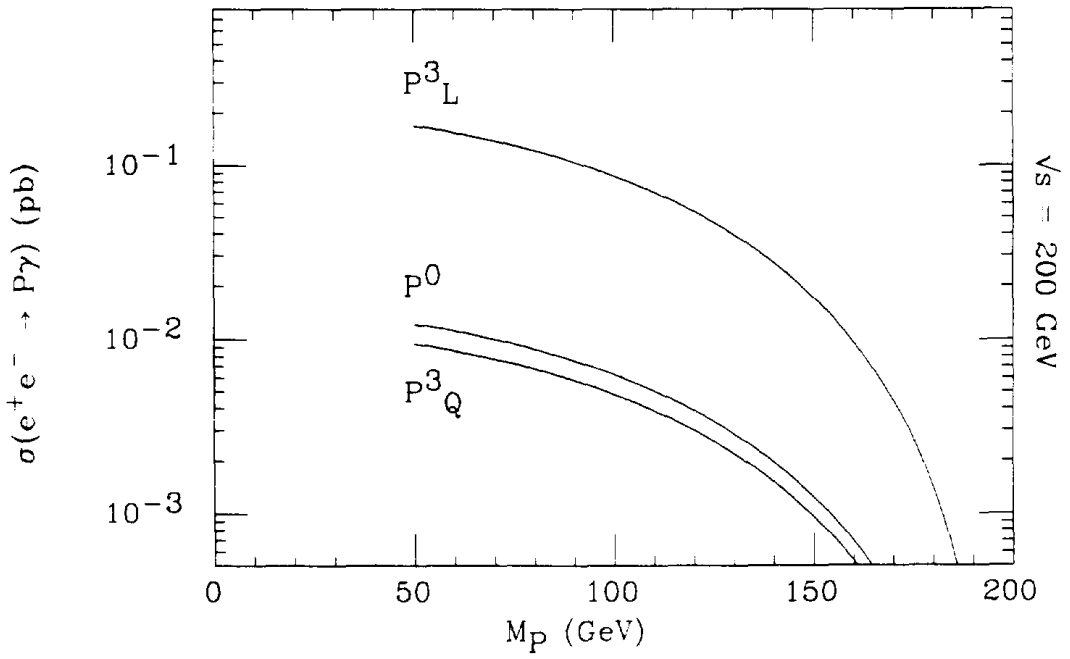

Fig. 4. The $\sigma(e^+e^- \to P\gamma)$ cross sections, in the LR model, as a function of the PGB mass M_P. The energy in the center of mass is fixed to the value of 200 GeV.

the anomalous couplings to the photons and Z^0 gauge bosons are quite close to their typical values of one. Therefore, a cross section of the order of 10^{-2} pb is a typical value expected in multiscale WTC models. We then conclude that, in order the PGBs can be produced at the LEP II experiment, in this channel, the corresponding $A_{PB_1B_2}$ coupling constants must be, in some of the relevant cases, larger than one. This can happen, and, in particular, this is just the case of the LR model of WTC.

The rate of PGB production, for the processes of Eq. (23), is expected to be significantly larger at a 500 GeV NLC experiment. For the three PGBs of the LR model, the values of the $\sigma(e^+e^- \to P\gamma)$ cross section are shown in Fig. 5, as a function of the PGB mass M_P. In the case of the PGB P_L^3, the cross section is of the order of 10^{-1} pb, in the whole range of masses typically expected for this particle. By assuming a luminosity of 10^4 pb^{-1}/yr, this means that the number of PGBs produced per year is approximately 10^3. In the case of the PGBs P_Q^3 and P^0 this number is then reduced by approximately one order of magnitude.

In the NLC experiment, the PGB production can also occur in the $e^+e^- \to PZ^0$ channel. Typically, in multiscale WTC models, the values of the corresponding cross sections are found to be between 10^{-2} and 10^{-3} pb, so that a considerable rate of PGB production can be expected also in this channel.

To make a comparison, we now consider the $e^+e^- \to PB$ processes in the framework of traditional, single scale, TC models. We remind that in this case the quantity $F_P\sqrt{n/2}$ is equal to 246 GeV, so that the only model dependence of the cross section in Eq. (24) comes from the number of technicolors N_{TC} and the values of the $A_{PB_1B_2}$ coupling

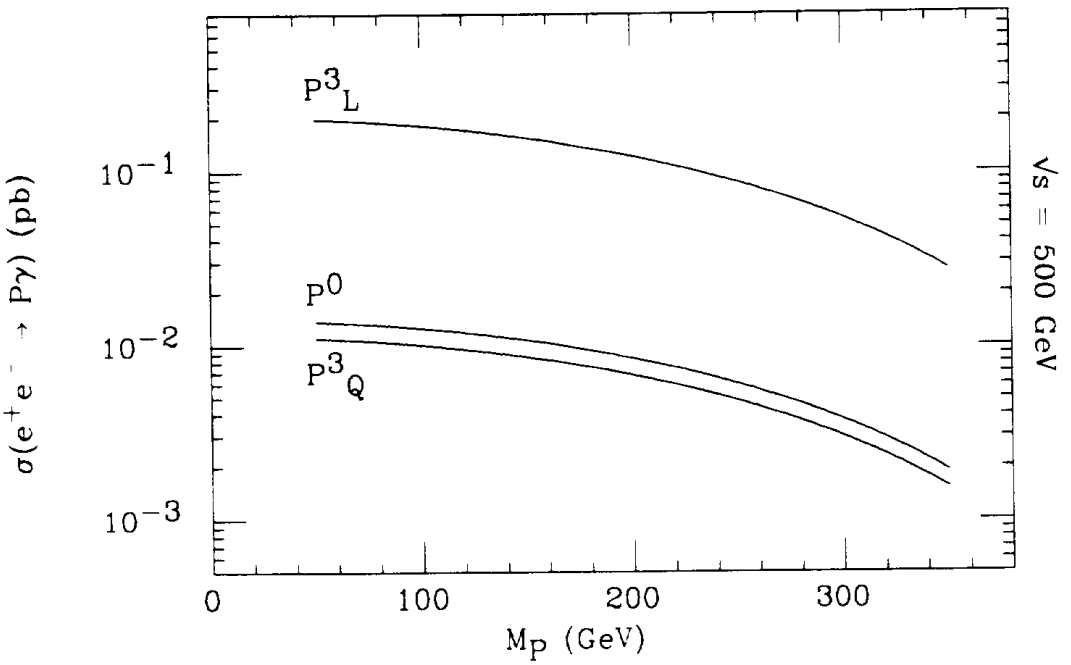

Fig. 5. The $\sigma(e^+e^- \to P\gamma)$ cross sections, in the LR model, as a function of the PGB mass M_P. The energy in the center of mass is fixed to the value of 500 GeV.

constants. In the one family FS model, for instance, all these constants are quite close to their typical value of one (see Table 3). In this case, even by assuming the large value $N_{TC} = 8$ and by considering PGB masses of the order of 50 GeV, we find that the total number of $e^+e^- \to P\gamma$ and $e^+e^- \to PZ$ events is expected to be approximately of only 10 per year at NLC, whereas no PGBs will be typically produced, in these channels, at the LEP II experiment.

4.3. *Analysis of the $e^+e^- \to P\gamma$ events at LEP II*

Let us now discuss, in some detail, the experimental signatures of the $e^+e^- \to P\gamma$ events and the predicted Standard Model background. To be specific, we will consider in this section the values of model parameters and couplings of the PGB P_L^3 of the LR model. In practice, the precise values of these couplings are not relevant for the following analysis, whose results can be applied, at least qualitatively, to any other model of WTC. In this respect, the only relevant assumption is that the model contains one PGB whose anomalous coupling with a photon pair is large enough for this particle to be produced at LEP II.

Let us first assume that the mass of the PGB is fixed to the value of 100 GeV. In this case, the main results of the analysis we are going to perform are summarized in Table 4.

At LEP II, the $\sigma(e^+e^- \to P_L^3\gamma)$ cross section, for the PGB P_L^3 with a mass of 100 GeV, is equal to approximately $0.87 \cdot 10^{-1}$ pb. This corresponds to a production

Table 4
Values of the cross sections (in pb), branching ratios and expected number of events per year for the $e^+e^- \to P_L^3\gamma$ processes and the relevant Standard Model background at the LEP II experiment. N_S and N_B refer to the signal and background respectively. For the "cut" see text. The PGB mass is fixed to the value M_P = 100 GeV

M_P = 100 GeV	$B_{Pff} = 1/3$	$B_{Pff} = 1$	$B_{Pff} = 3$
$\sigma(e^+e^- \to P\gamma)$	$0.87 \cdot 10^{-1}$	$0.87 \cdot 10^{-1}$	$0.87 \cdot 10^{-1}$
$Br(P \to \bar{b}b)$	0.34	0.75	0.86
$Br(P \to \gamma\gamma)$	0.61	0.15	0.02
$\sigma_S(e^+e^- \to \bar{b}b\gamma)_{\rm cut}$	$0.27 \cdot 10^{-1}$	$0.59 \cdot 10^{-1}$	$0.68 \cdot 10^{-1}$
$N_S(e^+e^- \to \bar{b}b\gamma)$	14	30	34
$N_B(e^+e^- \to \bar{b}b\gamma)$	10	10	10
$\sigma_S(e^+e^- \to \gamma\gamma\gamma)_{\rm cut}$	$0.43 \cdot 10^{-1}$	$0.10 \cdot 10^{-1}$	$0.01 \cdot 10^{-1}$
$N_S(e^+e^- \to \gamma\gamma\gamma)$	21	5	1
$N_B(e^+e^- \to \gamma\gamma\gamma)$	6	6	6

rate of more than 40 PGBs per year. The P_L^3 is then expected to decay mainly into a $\bar{b}b$ or into a $\gamma\gamma$ pair. As the ETC coupling constants, B_{Pff}, increase from 1/3 to 3, the corresponding branching ratios vary between 34% and 86% in the $\bar{b}b$ channel, and between 61% and 2% for the decay into a photon pair.

If the PGB decays into a pair of bottom quarks, then the expected signal is an event with two high energy, well isolated, jets and a monochromatic photon.

Up to small corrections, of $O(m_b^2/M_P^2)$, the minimum energy of each jet is equal to $M_P^2/4E$ = 25 GeV, where E=100 GeV is the energy of the electron beam. In addition, the two jets are separated by an angle, θ_{bb}, that is always larger than the minimum value $\theta_{bb}^{\rm min} = \arccos(2\beta_P^2 - 1)$, where $\beta_P = (4E^2 - M_P^2)/(4E^2 + M_P^2)$ is the speed of the PGB. In the case we are considering, $\beta_P = 0.6$ and $\theta_{bb}^{\rm min} \simeq 106^\circ$.

The main signature of these events is the presence of a monochromatic photon, whose energy is given by:

$$E_\gamma = E - \frac{M_P^2}{4E} = 75 \text{ GeV} \tag{25}$$

Thus, the behaviour of the differential cross section, $d\sigma/dE_\gamma$, is represented, for the signal, by a sharp peak in correspondence of this energy.

The finite width of the peak is determined by three effects. The uncertainty on the beam energy, the experimental error in the measure of the photon energy and the physical width of the PGB. In this analysis we assume that, at the LEP II experiment, the uncertainty on the beam energy will be equal to ΔE = 30 MeV, and the accuracy in measuring the photon energy will be $\Delta E_\gamma/E_\gamma$ = 1.2%. As far as the PGB width is concerned, its value can vary considerably with the values of the ETC constants B_{Pff}. If these constants are assumed to be all equal, then we find that Γ_P can vary between 13

MeV, for $B_{Pff} = 1/3$, and 420 MeV, for $B_{Pff} = 3$. Thus, the ratio Γ_P/M_P is expected to be at most of the order of $4 \cdot 10^{-3}$. We then find that the width of the peak, in the shape of $d\sigma/dE_\gamma$, turns out to be mainly determined by the experimental error in the measure of the photon energy, and it is expected to be equal to approximately 1 GeV.

Within the Standard Model, the total $e^+e^- \to \bar{q}q\gamma$ cross section has been computed, to the lowest order in perturbation theory, in Ref. [27]. This cross section turns out to be divergent when the final photon becomes collinear with the beam direction. Thus, in order to compute the expected background, we have applied the cut $20^\circ \leq \theta_{\gamma e} \leq 160^\circ$ on the angle between the photon and the initial electrons. In addition, according to Eq. (25) and the estimated value of Γ_P, we have only considered photons with energy between 74 and 76 GeV. In this way, we find that, in the Standard Model, the $\sigma(e^+e^- \to \bar{b}b\gamma)$ background cross section, for $\sqrt{s} = 200$ GeV, is equal to approximately $2 \cdot 10^{-2}$ pb. This corresponds, at LEP II, to 10 events per year.

The differential cross section, $d\sigma/d\cos\theta_{\gamma e}$, for the $e^+e^- \to P_L^3\gamma$ events, is proportional to $1 + \cos^2\theta_{\gamma e}$. Thus, the above cuts on the angle $\theta_{\gamma e}$ implies the loss of approximately 9% of the signal. We then find that the number of PGB expected per year in this channel varies from 14, for $B_{Pff} = 1/3$, to 34, for $B_{Pff} = 3$ (see Table 4). The ratio signal/background is therefore equal to 1.4, when $B_{Pff} = 1/3$, and it is always larger than 3 if B_{Pff} is larger than 1. Thus, these events are expected to be clearly distinct from the Standard Model background.

In order to estimate the number of events that can be effectively observed at LEP II, we must finally consider the experimental efficiency in detecting b quarks. In these events, at least one of the two final b quarks must be reconstructed, and the corresponding efficiency can be assumed to be of the order of 65%, if the purity of the sample is approximately 85%. Thus, in the case of the PGB P_L^3, we find that more than 20 events per year can be observed at LEP II, in the $e^+e^- \to P_L^3\gamma \to \bar{b}b\gamma$ channel, provided the ETC coupling constants are equal or larger than one.

If the ETC coupling constants are smaller than one, then the PGB P_L^3 is expected to decay mainly into a photon pair. For $M_P = 100$ GeV and $B_{Pff} = 1/3$, the $P_L^3 \to \gamma\gamma$ branching ratio is equal to 61%. In this case, the WTC event is characterized by the spectacular signature of only three photons in the final state. One of these photons has energy that is still given by Eq. (25), and the other two have energies larger than 25 GeV.

In the Standard Model, the $\sigma(e^+e^- \to 3\gamma)$ cross section has been calculated in Ref. [28], in the limit of vanishing electron mass. By using their results, we have computed the value of this cross section by requiring at least one photon with an energy between 74 and 76 GeV, and the two other photons with energies larger than 25 GeV. In order to avoid collinear divergences, we have also required the angles between the photons and the electron beam to be always in the range between 20 and 160 degrees. With these cuts, we find that, in the Standard Model, the $\sigma(e^+e^- \to 3\gamma)$ background cross section is equal to approximately $1.2 \cdot 10^{-2}$ pb, corresponding, at LEP II, to 6 events per year.

By performing a simple Monte Carlo simulation, we have estimated that the above

MeV, for $B_{Pff} = 1/3$, and 420 MeV, for $B_{Pff} = 3$. Thus, the ratio Γ_P/M_P is expected to be at most of the order of $4 \cdot 10^{-3}$. We then find that the width of the peak, in the shape of $d\sigma/dE_\gamma$, turns out to be mainly determined by the experimental error in the measure of the photon energy, and it is expected to be equal to approximately 1 GeV.

Within the Standard Model, the total $e^+e^- \to \bar{q}q\gamma$ cross section has been computed, to the lowest order in perturbation theory, in Ref. [27]. This cross section turns out to be divergent when the final photon becomes collinear with the beam direction. Thus, in order to compute the expected background, we have applied the cut $20^\circ \leq \theta_{\gamma e} \leq 160^\circ$ on the angle between the photon and the initial electrons. In addition, according to Eq. (25) and the estimated value of Γ_P, we have only considered photons with energy between 74 and 76 GeV. In this way, we find that, in the Standard Model, the $\sigma(e^+e^- \to \bar{b}b\gamma)$ background cross section, for $\sqrt{s} = 200$ GeV, is equal to approximately $2 \cdot 10^{-2}$ pb. This corresponds, at LEP II, to 10 events per year.

The differential cross section, $d\sigma/d\cos\theta_{\gamma e}$, for the $e^+e^- \to P_L^3\gamma$ events, is proportional to $1 + \cos^2\theta_{\gamma e}$. Thus, the above cuts on the angle $\theta_{\gamma e}$ implies the loss of approximately 9% of the signal. We then find that the number of PGB expected per year in this channel varies from 14, for $B_{Pff} = 1/3$, to 34, for $B_{Pff} = 3$ (see Table 4). The ratio signal/background is therefore equal to 1.4, when $B_{Pff} = 1/3$, and it is always larger than 3 if B_{Pff} is larger than 1. Thus, these events are expected to be clearly distinct from the Standard Model background.

In order to estimate the number of events that can be effectively observed at LEP II, we must finally consider the experimental efficiency in detecting b quarks. In these events, at least one of the two final b quarks must be reconstructed, and the corresponding efficiency can be assumed to be of the order of 65%, if the purity of the sample is approximately 85%. Thus, in the case of the PGB P_L^3, we find that more than 20 events per year can be observed at LEP II, in the $e^+e^- \to P_L^3\gamma \to \bar{b}b\gamma$ channel, provided the ETC coupling constants are equal or larger than one.

If the ETC coupling constants are smaller than one, then the PGB P_L^3 is expected to decay mainly into a photon pair. For $M_P = 100$ GeV and $B_{Pff} = 1/3$, the $P_L^3 \to \gamma\gamma$ branching ratio is equal to 61%. In this case, the WTC event is characterized by the spectacular signature of only three photons in the final state. One of these photons has energy that is still given by Eq. (25), and the other two have energies larger than 25 GeV.

In the Standard Model, the $\sigma(e^+e^- \to 3\gamma)$ cross section has been calculated in Ref. [28], in the limit of vanishing electron mass. By using their results, we have computed the value of this cross section by requiring at least one photon with an energy between 74 and 76 GeV, and the two other photons with energies larger than 25 GeV. In order to avoid collinear divergences, we have also required the angles between the photons and the electron beam to be always in the range between 20 and 160 degrees. With these cuts, we find that, in the Standard Model, the $\sigma(e^+e^- \to 3\gamma)$ background cross section is equal to approximately $1.2 \cdot 10^{-2}$ pb, corresponding, at LEP II, to 6 events per year.

By performing a simple Monte Carlo simulation, we have estimated that the above

Table 6
Same as in Table 4, but with the PGB mass fixed to the value $M_P = 150$ GeV

$M_P = 150$ GeV	$B_{Pff} = 1/3$	$B_{Pff} = 1$	$B_{Pff} = 3$
$\sigma(e^+e^- \to P\gamma)$	$0.17 \cdot 10^{-1}$	$0.17 \cdot 10^{-1}$	$0.17 \cdot 10^{-1}$
$Br(P \to \bar{b}b)$	0.19	0.63	0.84
$Br(P \to \gamma\gamma)$	0.78	0.28	0.04
$\sigma_S(e^+e^- \to \bar{b}b\gamma)_{\text{cut}}$	$0.03 \cdot 10^{-1}$	$0.10 \cdot 10^{-1}$	$0.13 \cdot 10^{-1}$
$N_S(e^+e^- \to \bar{b}b\gamma)$	2	5	7
$N_B(e^+e^- \to \bar{b}b\gamma)$	1	1	1
$\sigma_S(e^+e^- \to \gamma\gamma\gamma)_{\text{cut}}$	$0.11 \cdot 10^{-1}$	$0.04 \cdot 10^{-1}$	$0.00 \cdot 10^{-1}$
$N_S(e^+e^- \to \gamma\gamma\gamma)$	5	2	0
$N_B(e^+e^- \to \gamma\gamma\gamma)$	3	3	3

coupling between the PGBs and the top quark pairs is of the standard form, i.e. m_t/F_P. In this case, in multiscale WTC models, this coupling is typically larger than one, and, a priori, it can play an important role in PGB production.

In order to investigate the role of the ETC interactions at the LEP II and NLC energies, we study the processes:

$$e^+e^- \to P\bar{f}f \tag{26}$$

in which $\bar{f}f$ is a fermion pair. The particular case of quasi-elastic scattering, $e^+e^- \to Pe^+e^-$, will be discussed separately in the following section.

In the processes of Eq. (26), the ETC interactions enter at the lowest order. The relevant Feynman diagrams are the eight diagrams represented in Fig. 6. In the first four diagrams, (A1) and (A2), the PGB in the final state is produced by the decay of a virtual gauge boson. Thus, these diagrams are still controlled by the anomalous couplings between PGBs and standard gauge bosons. In contrast, in the last four diagrams, (B1) and (B2), the technipion is emitted by one of the two fermions produced in the final state, and the production of the PGBs occurs via the ETC interactions.

The calculation of the $\sigma(e^+e^- \to P\bar{f}f)$ cross section has been performed by neglecting the small masses of the electrons in the initial state.

In the limit in which the finite lifetime of the Z^0 gauge boson is also neglected, the total cross section turns out to be divergent, due to the contribution of the two diagrams, labeled as (A1) in Fig. 6, in which the virtual Z^0, decaying in the final fermion pair, can be produced on shell. In order to avoid these divergences, a finite Z^0 lifetime has been taken into account.

The same kind of divergences would also appear, in the calculation of the total cross section, if one neglects the mass of the final fermion pair. Indeed, in this limit also the virtual photon, entering in the diagrams (A2) of Fig. 6, can be produced on shell. In our calculation, the final fermion masses have been always taken into account. In addition,

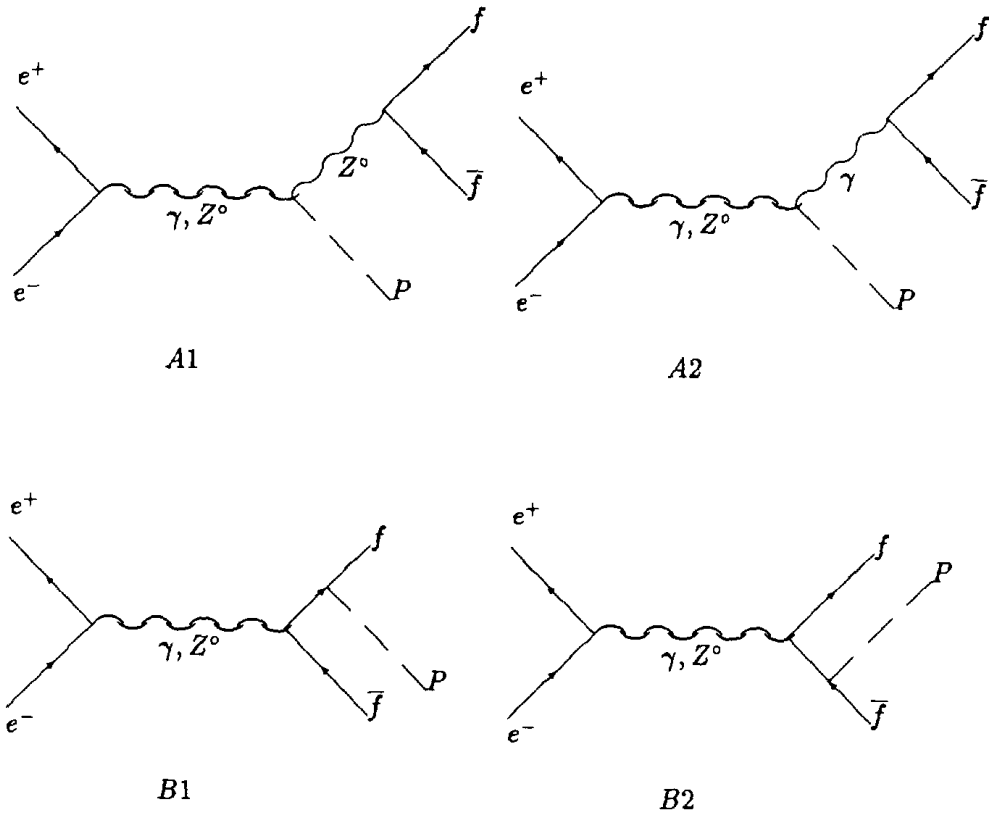

Fig. 6. Feynman diagrams relevant for the processes $e^+e^- \to P\bar{f}f$ in a model of ETC.

for light and massless final leptons (muons and neutrinos), we have imposed a lower cut on the values of the pair invariant mass, $M_{ff} \geq 1$ GeV.

The results of our calculation show that, at the future lepton collider experiments, the contributions of the several $e^+e^- \to P\bar{f}f$ channels to the total cross section of PGB production are quite small. For instance, at the energy of 200 GeV, the values of these cross sections in the LR model are smaller than 10^{-3} pb, corresponding, at LEP II, to less than one event per year in each channel. In order to observe these processes at LEP II, a cross section larger by approximately two order of magnitude would be required, and it is unlikely that this can be achieved in different WTC models.

At the NLC experiment, the $\sigma(e^+e^- \to P\bar{f}f)$ cross sections are found to be approximately of the same order of magnitude, but the luminosity of this machine is expected to be much higher than the luminosity at LEP II. However, it is still unlikely for these processes to be observed. As an example, we show in Fig. 7 the values of these cross sections as a function of the PGB mass M_P, for $\sqrt{s} = 500$ GeV and for the PGB P_L^3 of the LR model. In the figure, we have considered the cases in which the final fermions are a $\bar{t}t$, $\bar{b}b$, $\mu^+\mu^-$ and $\bar{\nu}\nu$ pair. The top quark mass is fixed to the value of 174 GeV. We see, from Fig. 7, that all the cross sections, are of the order, or smaller, than 10^{-3} pb, corresponding, at NLC, to a production rate of only few tenths of events per year.

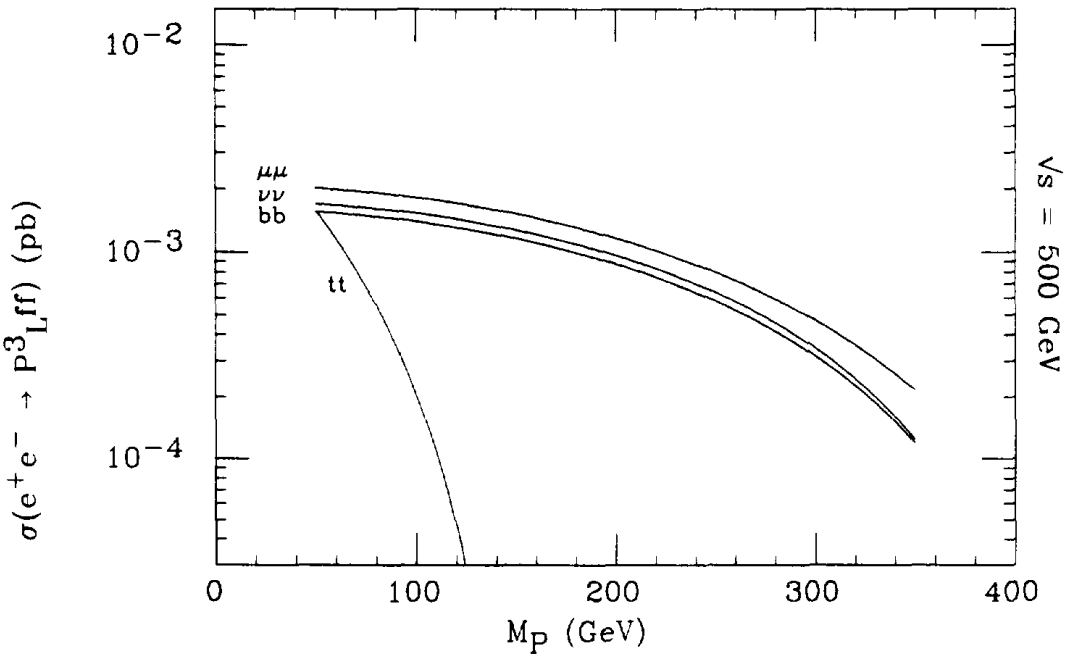

Fig. 7. The $\sigma(e^+e^- \to P^3_L \bar{f}f)$ cross section, in the LR model, as a function of the PGB mass M_P. The energy in the center of mass is fixed to the value of 500 GeV.

This rate is then found to be reduced by approximately one order of magnitude for the two PGBs P^3_Q and P^0, whose anomalous TC couplings are of the order of one. We also find that, via the processes considered in this section, there is no possibility, for the PGBs of traditional models, to be observed both at LEP II and the NLC experiments.

Fig. 7 shows that in all the different final states, by neglecting the case of final top quarks, the PGBs are produced with approximately the same probability. This feature reflects the fact that the PGB production, in these channels, mainly proceeds via the TC anomalous interactions. Indeed, the contribution of the ETC diagrams, (B1) and (B2) of Fig. 6, grows proportionally to the square of the fermion mass. In these processes, the only case in which the ETC interactions become relevant is the $e^+e^- \to P\bar{t}t$ channel. However, as results from Fig. 7, at NLC this channel is still strongly suppressed.

4.5. *The production of PGBs in the $e^+e^- \to Pe^+e^-$ channel*

When we consider, among the $e^+e^- \to P\bar{f}f$ processes of the previous section, the particular case in which an electron-positron pair is produced in the final state, four new Feynman diagrams enter, at the lowest order, in the calculation of total cross section. In these diagrams, represented in Fig. 8, the PGB is produced by the annihilation of two virtual gauge bosons, created by the initial electron and positron respectively. These virtual particles can be either photons or Z^0 gauge bosons[2].

[2] Similar diagrams, to those reported in Fig. 8, can also describe the $e^+e^- \to P\bar{\nu}\nu$ channel, that proceeds through the annihilation of a virtual $W^\pm$ pair. However, since the neutral isoscalar and isovector PGBs are not coupled to $W^\pm$ gauge bosons, we will not discuss this channel.

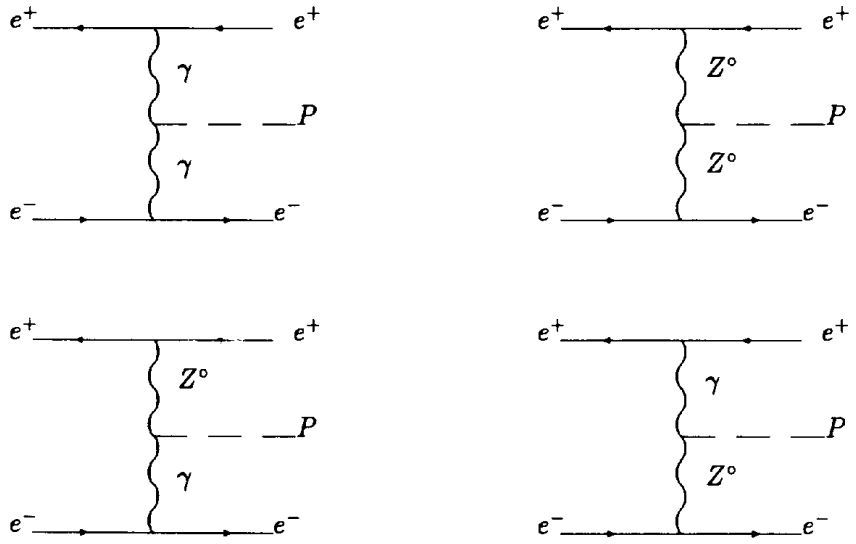

Fig. 8. Feynman diagrams relevant for the $e^+e^- \to Pe^+e^-$ channel.

In the limit in which the electron mass is neglected, several sources of collinear divergences appear in the calculation of the total cross section, coming from those diagrams of Fig. 8 containing at least one photon propagator. The degree of these divergences can be linear or logarithmic.

The effect of the collinear divergences, that, in the actual calculation are removed by the finite value of the electron mass, is, however, an enhancement of the resulting cross section. For this reason, we have neglected, in considering this channel, the contribution, to the total cross section, coming from the interference between the four diagrams of Fig. 8 and the eight diagrams considered in the previous section. In addition, we have found that, because of these collinear divergences, the PGB production in the $e^+e^- \to Pe^+e^-$ channel, receives the main contribution from the first diagram in Fig. 8, contribution that typically accounts for more than 95% of the total cross section.

In the limit in which only this contribution is taken into account, the total cross section can be written down in a very compact form. For these two-photon processes, a convenient procedure to perform the integration on the final phase space is explained in detail in Ref. [31]. By indicating with p_i and q_i $(i = 1,2)$ the four momenta of the initial and final electrons, and with $l_i = p_i - q_i$ the momenta of the two virtual photons, one finds:

$$\sigma_{\gamma\gamma}(e^+e^- \to Pe^+e^-) = \left(\frac{A_{P\gamma\gamma} N_{TC} \alpha^2}{2\sqrt{2}\pi^2 F_P \sqrt{n/2}}\right)^2 \int_{-C_L}^{+C_L} d(\cos\theta_1) \int_{-C_L}^{+C_L} d(\cos\theta_2)$$
$$\times \int_0^{2\pi} d\varphi \int_{M_P}^{E+M_P^2/4E} \frac{d\omega}{\sqrt{\omega^2 - s_0}} \frac{\vartheta(\omega^2 - s_0)}{1 - \cos\theta} \frac{\left(E^2 - E\omega + s_0/4\right)}{E^2} \frac{B}{\left(l_1^2 l_2^2\right)^2} \tag{27}$$

In this formula, θ_i represents the angle between initial and final electrons or positrons,

$\hat{p}_i \cdot \hat{q}_i = \cos\theta_i$, and θ is the angle between the two final leptons, $\cos\theta = \hat{q}_1 \cdot \hat{q}_2 = \sin\theta_1 \sin\theta_2 \cos\varphi - \cos\theta_1 \cos\theta_2$. The variable ω represents the energy of the PGB P and s_0 is given by:

$$s_0 = \frac{2M_P^2 + 4\left(E^2 - E\omega\right)(1+\cos\theta)}{1-\cos\theta} \tag{28}$$

The energies of the final leptons, E_1 and E_2 are expressed, in terms of ω and s_0, through the relations $E_{1,2} = E - (\omega \pm q)/2$, where $q = \sqrt{\omega^2 - s_0}$. Finally, the function B comes from the square of the Feynman amplitude, and has the form:

$$B = \tfrac{1}{4} l_1^2 l_2^2 B_1 - 4 B_2^2 + m_e^2 B_3 \tag{29}$$

with:

$$\begin{aligned}
B_1 &= (4 p_1 \cdot p_2 - 2 p_1 \cdot l_2 - 2 p_2 \cdot l_1 + l_1 \cdot l_2)^2 \; + + \; (l_1 \cdot l_2)^2 \; - \; l_1^2 l_2^2 \; - \; 16 m_e^4 \\
B_2 &= (p_1 \cdot p_2)(l_1 \cdot l_2) \; - \; (p_1 \cdot l_2)(p_2 \cdot l_1) \\
B_3 &= l_1^2 (2 p_1 \cdot l_2 - l_1 \cdot l_2) \; + \; l_2^2 (2 p_2 \cdot l_1 - l_1 \cdot l_2) \; + \; 4 m_e^2 (l_1 \cdot l_2)^2
\end{aligned} \tag{30}$$

The total cross section, in Eq. (27), receives the main contribution from the region of very small angles θ_i, where, in the limit of vanishing electron masses, the collinear divergences appear. However, since this kinematical configuration could be not easily accessible to the experimental observation, in Eq. (27) the cut $|\cos\theta_i| \leq C_L$ has been introduced ($C_L = 1$ for the total cross section). In our numerical calculations, we have always considered the case $\theta_i \geq 10^\circ$ ($C_L \simeq 0.9848$). This condition reduces the total cross section by approximately one order of magnitude.

The four dimensional integration in Eq. (27), or, in general, for the complete set of diagrams of Fig. 8, can be performed numerically. For the particular case of the LR model, the values of the $\sigma(e^+e^- \to Pe^+e^-)$ cross section are shown in Fig. 9 as a function of the PGB mass. The total energy in the center of mass is fixed, in the figure, at the LEP II value of 200 GeV. We see, from the figure, that for the PGB P_L^3 the values of this cross section turn out to be of the order of 10^{-2} pb, for almost any value of the PGB mass between 100 and 150 GeV. We also find that, in the cases of the two PGBs P^0 and P_Q^3, this rate is reduced by approximately one order of magnitude.

Thus, in the LR model, the production rate of PGBs, in the $e^+e^- \to Pe^+e^-$ channel, is expected to be of the order of few events per year, and it is unlikely that these events could be observed at LEP II. Since the cross section is dominated by the contribution of the first diagram in Fig. 8, its value scales essentially like the ratio $(A_{P\gamma\gamma} N_{TC}/F_P\sqrt{n/2})^2$, as results from Eq. (27). In this ratio is contained all the model dependence of this cross section. Therefore, a larger production can be predicted in the framework of different WTC models (e.g. models with a smaller TC scale or a larger value of N_{TC}). Since the results of Fig. 9 turn out to be probably at the limit of a possible experimental observation, we then believe that even this channel is worth an experimental research.

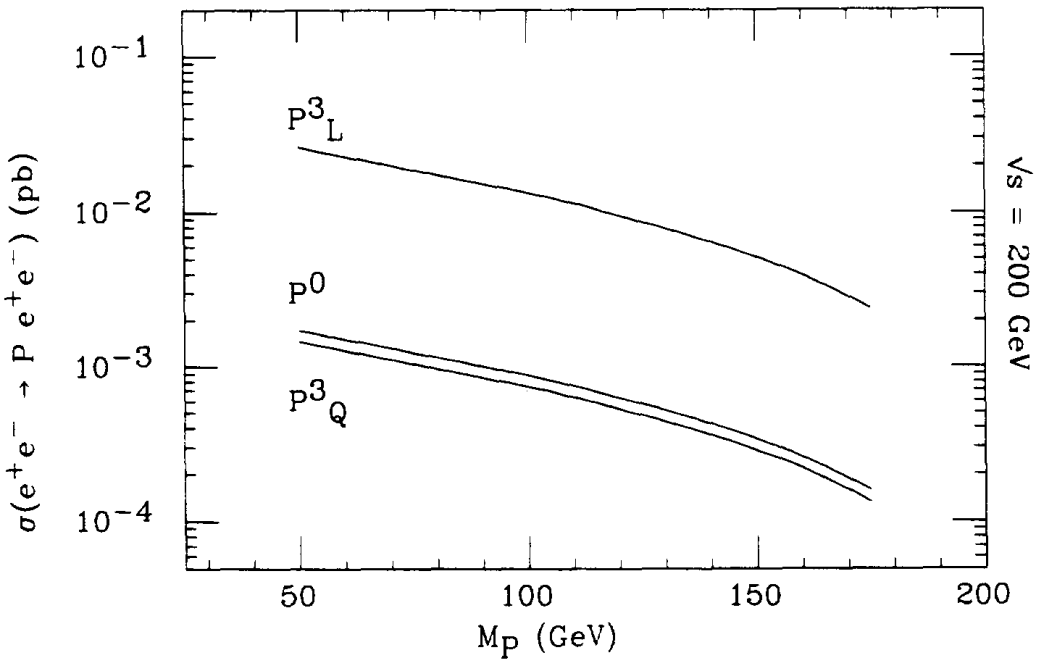

Fig. 9. Values of the $\sigma(e^+e^- \to Pe^+e^-)$ cross sections, in the LR model, as a function of the PGB mass M_P. The energy in the center of mass is fixed to the value of 200 GeV.

In particular, a clear signal of the $e^+e^- \to Pe^+e^-$ events would occur if the produced PGB decays into a photon pair. According to our previous results, this is expected to be the favored decay mode when the ETC coupling between the PGB and a bottom pair is smaller than one. In this case, the WTC events would be characterized, in the final state, by an electron pair, typically emitted at small angles with respect to the direction of the initial beam, and by a high energetic photon pair. Each of the photons will have energy larger than $M_P^2/4E$, where E is the energy of the electron beam (this means $E_\gamma \geq 25$ GeV, for $M_P \geq 100$ GeV). In addition, the photon pair will be monochromatic, with an invariant mass equal to the PGB mass.

We have estimated that, for these events, the expected Standard Model background, at LEP II, would be completely negligible, typically smaller by one order of magnitude with respect to the signal.

In order to compute the signal/background ratio, we have used a Monte Carlo event generator, kindly provided us by the authors of Ref. [32]. With this code, for any considered value of the PGB mass, we have computed the number of Standard Model $e^+e^- \to e^+e^-\gamma\gamma$ events, in which the photon pair invariant mass turns out to be in the range between $M_P - \Delta M$ and $M_P + \Delta M$, where ΔM represents the experimental uncertainty in the measure of the photon invariant mass. The value of ΔM is determined by both the uncertainty in the measure of the single photon energy, that we have assumed to be equal to $\Delta E_\gamma/E_\gamma = 1.2\%$, and the uncertainty in the measure of the angle between the two photons, that we have considered to be $\Delta\theta_{\gamma\gamma} = 0.5°$. At LEP II, ΔM is dominated by the former uncertainty, and we find $\Delta M/M \simeq 1\%$.

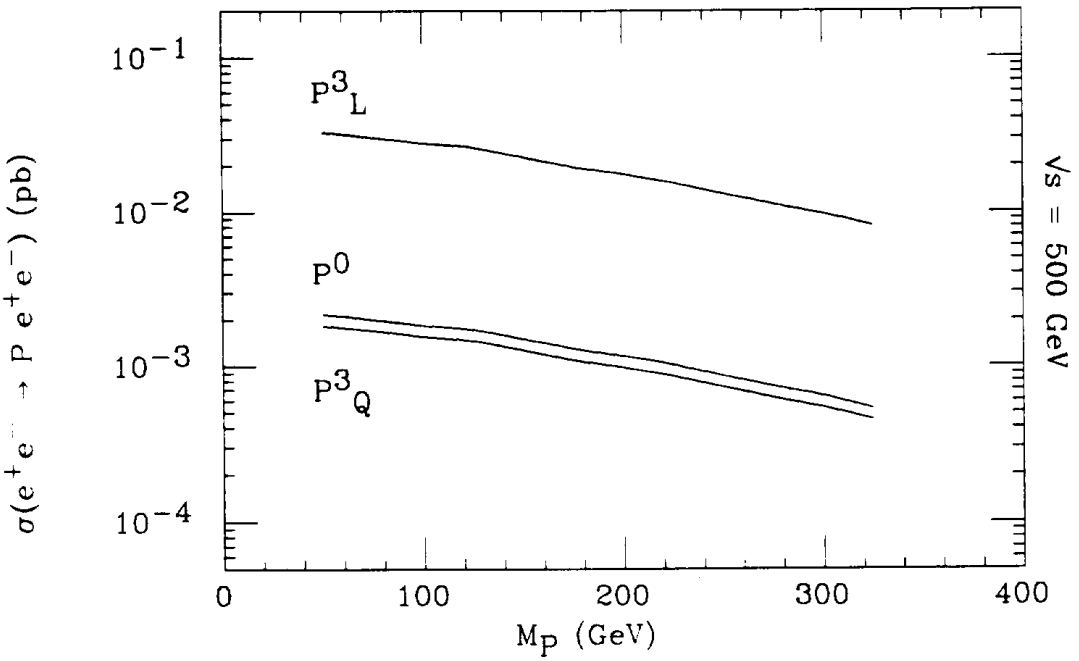

Fig. 10. The $\sigma(e^+e^- \to Pe^+e^-)$ cross sections, in the LR model, as a function of the PGB mass M_P. The energy in the center of mass is fixed to the value of 500 GeV.

In order to avoid collinear divergences and to select clear events, in computing the Standard Model background cross section we also have required final leptons with energy greater than 3 GeV and all the particles well separated by an angle of at least 10°. These cuts, applied to the signal, reduces the corresponding cross sections of approximately 15%. Finally, we have imposed, on the Standard Model background, the same kinematical constraint of the signal events, namely final leptons with energy smaller than $E - M_P^2/4E$, and a lepton pair invariant mass smaller than $2E - M_P$.

After all these cuts have been imposed, we find that the $\sigma(e^+e^- \to e^+e^-\gamma\gamma)$ cross section, in the Standard Model, reduces to approximately 10^{-3} pb, corresponding at LEP II to less than 1 event per year. Thus, in this channel, the TC events are expected to be practically free of Standard Model background.

At a 500 GeV NLC experiment, the values of the $\sigma(e^+e^- \to Pe^+e^-)$ cross sections are found to be in the range between 10^{-2} and 10^{-3} pb. For the particular case of the LR model, these values are shown in Fig. 10 (they have been computed by always requiring a minimum angle of 10° between initial and final leptons). Thus, we expect a number of events per year of the order of several hundreds.

Finally, we find that, within the framework of traditional TC models, only few events per year can be expected, in this channel, at the NLC experiment, by assuming standard couplings of the order of one as in the case of the FS model. Moreover, no PGBs of traditional TC models are typically predicted to be produced at LEP II experiment.

5. Conclusions

We now summarize the main results of this paper and present our conclusions.

The existence of a large number of PGBs is a quite general prediction of any TC/ETC model. In multiscale WTC theories, the lightest of these states have masses that are typically expected to be larger than 100 GeV. In this paper, we have studied the production and decay of such particles at the high energy e^+e^- experiments, LEP II and NLC.

The couplings of neutral PGBs, to ordinary fermions and gauge bosons, can be written in a form that is, to some extent, model independent. All the model dependence is explicitly included in the values of the pseudoscalar decay constants of technipions, in the dimension of the TC gauge group, N_{TC}, and in two classes of model dependent couplings, which, however, are typically expected to be of order one. Thus, we are able to study quite general predictions of the theory for the various production and decay rates.

Our results show that, in multiscale WTC theories, because of the existence of relatively low TC scales, the production of neutral PGBs, in e^+e^- collisions, is significantly enhanced. The corresponding cross sections are expected to be larger, by one or two orders of magnitude, with respect to the predictions of traditional single-scale TC models. Thus, despite the typically large values of PGB masses, these particles could be observed even at the energy and luminosity of the LEP II experiment.

As an example, we have shown that this production is indeed expected to occur in the LR model of WTC, provided the PGB masses are not larger than approximately 150 GeV. In general, a typical condition for this production to occur at LEP II, with a significant rate, is that the anomalous coupling of the neutral PGB with a photon pair is larger than one ($A_{P_l^3\gamma\gamma} \sim 7$ in the LR model).

At LEP II, the main contributions to the PGB production is expected to come from the $e^+e^- \to P\gamma$ channel, and, possibly, with a smaller rate, from the $e^+e^- \to Pe^+e^-$ channel. For isovector PGBs, we find that the relevant decay modes are predicted to be into a bottom quark or a photon pair. In particular, the $P \to \gamma\gamma$ decay is a typical signature of WTC dynamics, since it turns out to be usually strongly suppressed in traditional TC models. At LEP II, in all the channels, by taking into account the experimental cuts and reconstruction efficiencies, we can expect a number of events of the order of several tenths per year, assuming an integrated luminosity of 500 pb^{-1}. We have also shown that, in most of the cases, the distinctive signatures of WTC events allow the Standard Model background to be reduced to a negligible level. Thus, these particles are worth of an experimental research.

At the NLC experiment, we expect that the production of neutral PGBs will be significantly larger, of the order of 10^3 events per year, assuming a total energy in the center of mass of 500 GeV and an integrated luminosity of 10^4 pb^{-1}. This production is predicted to occur mainly in the $e^+e^- \to P\gamma$, $e^+e^- \to PZ^0$ and $e^+e^- \to Pe^+e^-$ channels. Instead, no PGBs are typically expected to be observed, both at LEP II and the NLC experiment, within the framework of traditional TC models.

Acknowledgments

We are very grateful to Ken Lane, for many interesting discussions on the subject of this paper and for a critical reading of a preliminary version of the manuscript. We are indebted to Luciano Maiani for having exhorted us to investigate this topic. Useful discussions with Franco Buccella and Marco Masetti have been also appreciated. We wish to thank Bing Zhou, for valuable discussions on the technical features of the LEP II experiment, and Ramon Miquel, for having provided us with a Monte Carlo generator of the $e^+e^- \to e^+e^-\gamma\gamma$ events in the Standard Model. V.L. acknowledges the support of an INFN post-doctoral fellowship.

References

[1] S. Weinberg, Phys. Rev. D 19 (1979) 1277.
[2] L. Susskind, Phys. Rev. D 20 (1979) 2619.
[3] E. Farhi and L. Susskind, Phys. Rep. 74 (1981) 277.
[4] S. Dimopoulos and L. Susskind, Nucl. Phys. B 155 (1979) 237.
[5] E. Eichten and K. Lane, Phys. Lett. B 90 (1980) 125.
[6] E. Eichten, I. Hinchliffe, K. Lane and C. Quigg, Phys. Rev. D 34 (1986) 1547; Rev. Mod. Phys. 56 (1984) 579.
[7] A. Manohar and L. Randall, Phys. Lett. B 246 (1990) 536.
[8] L. Randall and E.H. Simmons, Nucl. Phys. B 380 (1992) 3.
[9] V. Lubicz, Nucl. Phys. B 404 (1993) 559.
[10] S. Dimopoulos and J. Ellis, Nucl. Phys. B 182 (1981) 505.
[11] M. Peskin and T. Takeuchi, Phys. Rev. Lett. 65 (1990) 964;
R.N. Cahn and M. Suzuki, Phys. Rev. D 44 (1991) 3641;
M. Peskin and T. Takeuchi, Phys. Rev. D 46 (1992) 381;
M. Golden and L. Randall, Nucl. Phys. B 361 (1991) 3;
B. Holdom and J. Terning, Phys. Lett. B 247 (1990) 88;
A. Dobado, D. Espriu and M.J. Herrero, Phys. Lett. B 255 (1990) 405;
R. Casalbuoni et al., Phys. Lett. B 258 (1991) 161;
H. Georgi, Nucl. Phys. B 363 (1991) 301.
[12] See for example P. Langacker, Theoretical Study of the Electroweak Interactions - Present and Future, in Proceedings 22nd INS Symposium on Physics with High Energy Colliders, Tokyo (March 1994).
[13] B. Holdom, Phys. Rev. D 24 (1981) 1441; Phys. Lett. B 150 (1985) 301;
T. Appelquist, D. Karabali and L.C.R. Wijewardhana, Phys. Rev. Lett. 57 (1986) 957;
K. Yamawaki, M. Bando and K. Matumoto, Phys. Rev. Lett. 56 (1986) 1335;
T. Appelquist and L.C.R. Wijewardhana, Phys. Rev. D 35 (1987) 774; D 36 (1987) 568.
[14] See for example K. Lane, Technicolor and Precision Tests of the Electroweak interactions, Invited talk given at the 27th International Conference on High Energy Physics, Glasgow (20-27th July 1994).
[15] R.S. Chivukula, M.J. Dugan and M. Golden, Phys. Lett. B 292 (1992) 435.
[16] T. Appelquist and G. Triantaphyllou, Phys. Lett. B 278 (1992) 345;
R. Sundrum and S. Hsu, Nucl. Phys. B 391 (1993) 127;
T. Appelquist and J. Terning, Phys. Lett. B 315 (1993) 139.
[17] K. Lane and M.V. Ramana, Phys. Rev. D 44 (1991) 2678.
[18] E. Farhi and L. Susskind, Phys. Rev. D 20 (1979) 3404.
[19] E. Eichten and K. Lane, Phys. Lett. B 222 (1989) 274.
[20] S. Dimopoulos, S. Rabi and L. Susskind, Nucl. Phys. B 169 (1980) 373.
[21] E. Eichten and K. Lane, Phys. Lett. B 327 (1994) 129.
[22] A. Manohar and H. Georgi, Nucl. Phys. B 234 (1984) 189;
H. Georgi and L. Randall, Nucl. Phys. B 276 (1986) 241.

[23] A.G. Cohen and H. Georgi, Nucl. Phys. B 314 (1989) 7.
[24] R. Dashen, Phys. Rev. 183 (1969) 183.
[25] J.S. Bell and R. Jackiw, Nuovo Cimento 60A (1969) 47;
S.L. Adler, Phys. Rev. 117 (1969) 2526.
[26] J. Ellis, M. Gaillard, D.V. Nanopoulos and P. Sikivie, Nucl. Phys. B 182 (1981) 529.
[27] M. Gourdin and F.M. Renard, Nucl. Phys. B 162 (1980) 285.
[28] F.A. Berends et al., Nucl. Phys. B 206 (1982) 61.
[29] F. Abe et al., CDF Collaboration, Phys. Rev. Lett. 73 (1994) 225; Phys. Rev. D 50 (1994) 2966.
[30] R.S. Chivukula, A.G. Cohen and K. Lane, Nucl. Phys. B 343 (1990) 554.
[31] S.J. Brodsky, T. Kinoshita and H. Terazawa, Phys. Rev. D 4 (1971) 1532.
[32] M. Martinez and R. Miquel, Phys. Lett. B 302 (1993) 108.